Manufacturing and Mechanical Characterization of Metal-Polymer-Metal Sandwich Composites.

By

Mr. Girma Worku

Roll No: RM0985/09

Faculty of Mechanical Engineering

Jimma Institute of Technology

Jimma University, Jimma.

Ethiopia.

A Thesis Submitted to Faculty of Graduate Studies of Jimma University in Partial Fulfillment of the Requirements for Degree of Masters of Science in Manufacturing Systems Engineering

December, 2019

Manufacturing and Mechanical Characterization of Metal-Polymer-Metal Sandwich Composites.

Post Graduate School of Mechanical Engineering

Jimma Institute of Technology
Jimma University

By: Mr. Girma Worku

Under the supervision of:

Advisor; Dr. Anil Kumar

Co-Advisor. Mr. Yegetaneh Tesfaye

A Thesis Submitted to School of Graduate Studies of Jimma University in Partial Fulfillment of the Requirements for Degree of Masters Science in Manufacturing Systems Engineering

December, 2019

JIMMA, ETHIOPIA

Declaration

I, undersigned and declare that this thesis is my original work, has not been presented for a degree in this or any other university and that all sources of materials used for the thesis have been fully acknowledged.

Name	Signature	Date
Girma Worku	_____	_____

Approval of the advisors

Advisor: Dr. Anil Kumar Signature _____ Date _____

Co advisor: Mr. Yegetane Tesfaye Signature_____ Date _____

This is to certify that the thesis prepared by Girma Worku, entitled: **"Manufacturing and Mechanical Characterization of Metal-Polymer Metal Sandwich Composites"** and submitted in partial fulfillment of the requirements for the degree of Master of Science in Manufacturing Systems Engineering compiles with the regulations of the University and meets the accepted standards with respect to originality and quality.
Signed by the Examining Committee:

Internal examiner	Signature	Date
_____	_____	_____
External examiner	Signature	Date
_____	_____	_____
Name of Chairman	Signature	Date
_____	_____	_____

Abstract

Metal-polymer-metal (MPM) sandwich composite consists of two or more metal sheets laminated hot pressed layer by layer with low strength of polymer material. To achieve enhanced mechanical properties of MPM materials exhibits high stiffness and strength, light weight, high plasticity, fire and vibration damping resistance. The general objective of this thesis is to manufacturing and experimental test to investigate mechanical properties of AA6061/HDPE/AA6061 sandwich sheets. Sandwich composite materials can be used in aeronautical, marine, automobile body, outer body of machines, refrigerator and air condition bodies, electrical device, house roofing and construction industrial applications. These materials help to reduce fuel consumption due to light weight and structural vibration damping resistance respectively. The significance of this study is to manufacture MPM sandwich material and introduce in Ethiopian industry as it is a new technology from advanced composite materials. This leads to increasing numbers of applications MPM composites for primary structural components. Three kinds of AA6061/HDPE/AA6061 sandwich sheet depend on the thicknesses of core materials will be prepared by the hot pressing method. Mechanical properties of three kinds sandwich sheets are investigated by conducting experimental tests, such as; tensile, hardness and density tests. Three-point bending, tensile strength, impact force and cohesive zone model for three kinds of sandwich sheets were analyses using ANSYS Workbench. For the present study high density polyethylene (HDPE) it was observed that the fabricated MPM sandwich composite materials were exhibiting better mechanical properties of these materials. By increasing the core thickness, the mechanical properties use improved.

Keywords*: Metal /polymer/metal sheets; AA6061 aluminum alloy, polyethylene and mechanical properties.*

Acknowledgment

Above all, I would like to thank the almighty God for being with me in all circumstance. Next, I am happy to acknowledge my advisor, Dr. Anil Kumar for his guidance from the beginning to the end of this work; I would love to thank My Co-Adivisor, Mr. Yegetaneh Tesfaye for his guidance, constant encouragement, and friendly approach throughout this thesis work. As an advisor, he provided me the inputs and guidance for this study. His support and patience throughout this research is sincerely appreciated.

And finally I would like to extend my special thanks to my families, friends, teachers, laboratory technicians and others who, directly or indirectly, understood on the side of me in support of best outcome of my work, even though I could not mention their best doing with such a few words. Thanks for never stop believing in me although Thanks for always pray for my success and happiness in the past, present and the future. Thanks for everything.

Table of contents

List of figures

List of tables

Abbreviations

ASTM: American standard test machine

CZM: Cohesive zone model

DOF: Degree of freedom

E_c: Elastic modules of core

E_m: Elastic modules of matrix

E_{sw}: Elastic modules of sandwich sheet

FLD: Flow Limit Diagram

FML: Fiber–Metal Laminates

GFRP: Glass Fiber Reinforcement Polymer

HDPE: High-Density Polyethylene

LDPE: Low-Density Polyethylene

LLDPE: Least Low-Density Polyethylene

MPM: Metal/polymer/metal

N.F. W: Natural fluorescent whitening agents

PE: Polyethylene

PP: polypropylene

SPS: Steel/polymer/steel

UTM: Universal testing machine

V_f : volume fraction of the matrix

V_m: volume fraction of the core

Chapter 1

Introduction

1.1 Background

Metal-polymer-metal (MPM) sandwich composite consists of two or more metal sheets laminated hot pressed layer by layer with low strength of polymer material. To achieve enhanced mechanical properties of MPM materials exhibits high stiffness and strength, high plasticity, fire and vibration damping resistance capacity of light polymer[1, 2].

On the other hand, customers have stringent demand for fuel economy with high performance at low cost [3]. In order to have high fuel economy, the auto-motive manufacturers are induced to reduce weight especially suitable for use in aeronautical, marine, automotive and civil engineering applications with the gradual requirement of fuel savings and structural weight reduction in industries [4, 5].

Over the past decades, metal- plastic sandwich sheets have generated a considerable interest as potential lightweight materials for structural parts due to the increasing demands for energy saving and better environmental impact of vehicles. Metal/polymer/metal (MPM) sandwich materials provide an innovative substitute for the used commercial sheets because of their lightweight potential with enhanced specific stiffness and thermal and acoustic isolation advantages [6].

Though, as a rule, consumers are more concerned with appearance, ergonomics, and comfort. At the same time, automobile engineer notices the modest technical performance of the structure. Undoubtedly, key factors of automobile volume production are cost, safety, volume production suitability, and universal reparability. Furthermore, different problems appeared in distinct phases of automobile history and their solutions often had an impact on body design fuel economy and protection of environment issues still engross minds of government organizations, corporations, and customers [7].

As there is a high emphasis on greenhouse gas reductions and improving fuel efficiency in the transportation sector, all car manufacturers, suppliers, assemblers, and component producers are investing significantly in lightweight materials research development and commercialization. All are moving towards the objective of increasing the use of lightweight materials and to obtain more market penetration by manufacturing components and vehicle structures made from lightweight materials. Because the single main obstacle in the application of lightweight materials is their high cost, priority is given to activities to reduce costs through the development of new materials, forming technologies, and manufacturing processes [8]. Some industrially applied metal Sandwich composite materials can be classified as follows:

a) Metal matrix natural polymers

Hybrid composite materials built up from interlacing layers of thin metals and natural fibers core. Natural fibers can be obtained from a plant, animal and mineral resources can be used as reinforcements in the manufacturing of green composite in the same way as the synthetic fibers, but it can be low-temperature operation and low formability compared to metal matrix thermoplastic polymer composites.

b) Metal matrix thermosetting fibre reinforced polymers

Fiber metal laminates are hybrid composite materials built up from interlacing layers of thin metals and fiber reinforced adhesives. The metal currently being used is either aluminum, magnesium or titanium, and the fiber-reinforced layer is either glass fiber, carbon fiber, and aramid fiber reinforced composite. They exhibit very good weight-specific stiffness and strength properties. The main problem with these products is their predominant brittleness so that they are strongly limited by their deformation processes [6,9].

c) Metal matrix thermoplastic polymers

Hybrid composite materials built up from interlacing layers of thin metals and thermoplastic adhesives. Materials have good formability for different sheet forming processes [6].

1.2 Statement of the Problem

The requirements of high strength, lightweight, vibration damping and corrosion resistance in aeronautical, marine, automobile body, outer body of machines, refrigerator and air condition bodies, electrical device, house roofing and construction industrial applications are becoming an impelling issue which needs to be answered. By improving a monolithic metallic sheet, into metal-plastic sandwich sheets. which offer light weight, higher specific flexural stiffness, fire and vibration damping resistances.

Especially in the automotive industry, the requirements for CO_2 emission reduction is becoming an impelling issue which needs to be answered, either by improving the performances of the engine or by reducing the weight of the vehicle. Concerning the latter, innovative a smart material can be utilized to replace the standard one, i.e. steel, and Aluminum to reduce the weight of the vehicle, thus increase the overall efficiency, while reducing the CO_2 emissions. These problem can get soliton the case of laminate MPM sandwich laminates which linked together by a thin layer of adhesive.

Generally, Among various sheet materials, the aluminum MPM sandwich sheets have generated a considerable interest as potential light-weight materials for the different applications; since its high specific strength, impact force resistance, vibration damping resistance and acoustic sound observation properties.

1.3 Significance of the study

The significance of this study is to manufacture MPM sandwich material and introduce in Ethiopian industry as it is a new technology from advanced composite materials. This leads to increasing numbers of applications MPM composites for primary structural components. To understand recycle thermoplastic for different applications and employed workers.

1.4 Objectives

1.4.1 General objective

- The general objective of this thesis is to manufacturing and experimental test to investigate the mechanical properties of MPM Sandwich composite materials for different Application.

1.4.2 Specific objectives

- To analyse mathematical model rule of mixture sandwich properties.
- Fabrication of MPM sandwich sheets by hot press method which has different thickness depends on the low strength of core polymer thickness at a constant thickness of high strength aluminum skin.
- To measure physical and mechanical experimental test of MPM sandwich properties using density, hardness and tensile tests.
- To analyse and simulation of tensile test, three-point bending, impact force resistance and cohesive zone model by ANSYS Workbench.

1.5 Methodology

The methodology of this thesis can be to determine good mechanical properties of sandwich laminates depend on the thickness of core materials. Shown from figure 1 the mechanical properties of MPM sandwich sheets can be analysis by experimental test and ANSYS Workbench simulation.

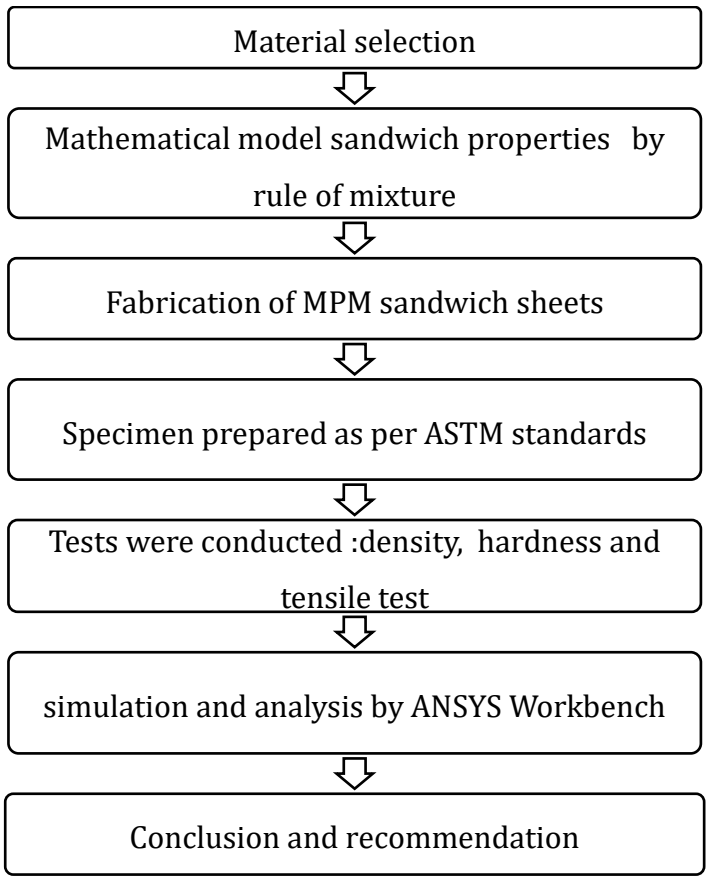

Figure 1. 1:The methodology of analysis AA6061/HDPE/ AA6061 sandwich laminates.

1.6 scope of the study

The scopes of this thesis are Study on composite material AA6061/HDPE/AA6061 sandwich laminates subject to different thickness under static load.

- To analyse mathematical model rule of mixture composite material for constant aluminum thickness.
- To measure physical properties using density tests.
- To measure mechanical properties using hardness and tensile tests.

- To analyse and simulation of tensile and flexural tests by ANSYS Workbench under static loads.
- To analyse and simulation of impact force resistance by ANSYS Workbench under dynamic explicitly.
- To analyse and simulation of prior damage and failure of cohesive bond by ANSYS Workbench under static load force Vs displacement.

1.7 limitation of the study

- Lack of availability experimental laboratory test composite material in Jimma University.
- Lack of hot pressing machine

1.8 Thesis organization

This work is organized into six chapters.

Chapter 1: Introduces the thesis background, problem of the statement, significance of the study, objectives, methodology, scope, and limitations.

Chapter 2: Literature review on composite materials, adhesion, mechanical Properties of MPM Sandwich Composites, literature review of modern composite materials and gap of research work.

Chapter 3: Aluminum-polymer laminates and experimental setup, rule of mixtures approach and material model characterization, fabrication of MPM sandwich sheets, experimental procedure, and setups.

Chapter 4: Modeling of mechanical property and finite element analysis, cohesive zone model and finite element analysis and cohesive zone model theory.

Chapter 5: Results and discussion, experimental and theoretical results, cohesive zone model simulation results and discussion

Chapter 6: Conclusions and recommendation.

Chapter 2

Literature review

The objective of this literature review to find the gap work from different sources such as; journal articles, encyclopedia articles, newspaper articles, books, and so on.

2.1 Composite materials

The composite material can be defined as a combination of two or more materials that results in better properties than those of the individual components used alone. In contrast to metallic alloys, each material retains its separate chemical, physical, and mechanical properties. They can be categorized according to their matrix phase and reinforcement are listed below [10].

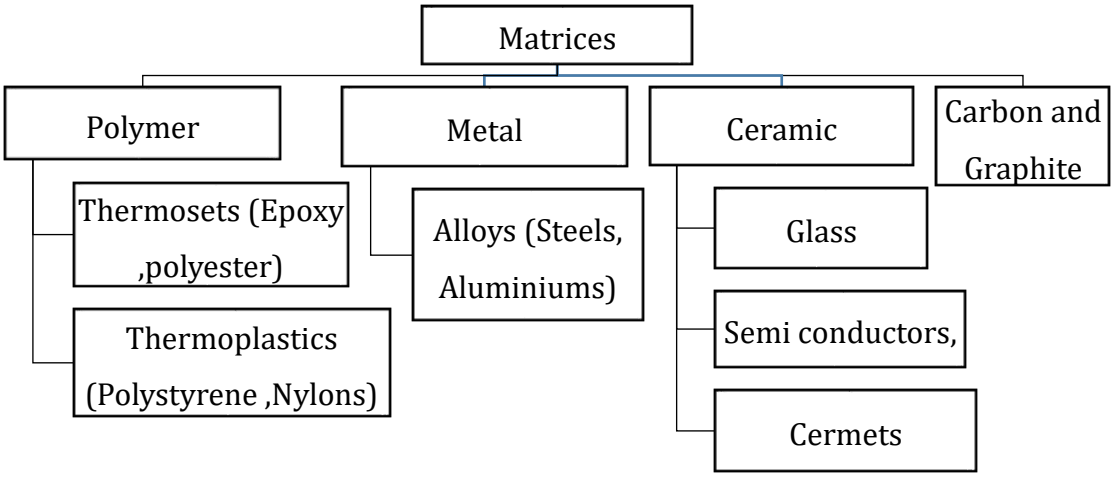

Figure 2. 1: Composite materials based on matrices phase.

Matrices are the continuous phase for the purposes to transfer stress to other phases and protect phases from the environment.

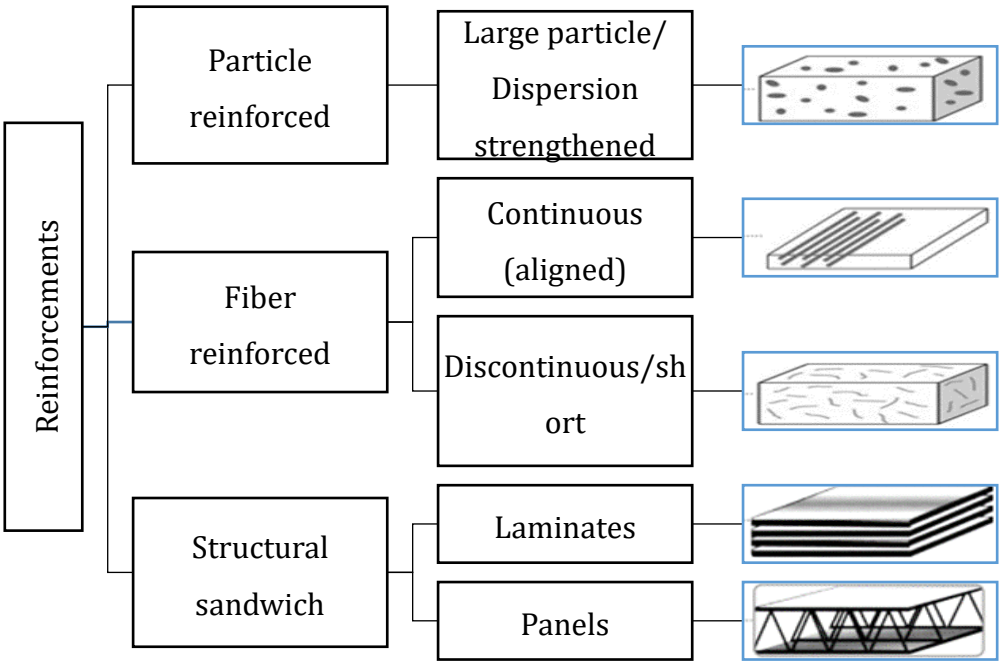

Figure 2. 2 :Composite materials based on reinforcements.

2.1.1 Ceramic matrix composite (CMC).

Ceramics exhibit attractive properties of high stiffness, hardness, compressive strength, and relatively low density. However; they are plagued by limitations of low toughness and bulk tensile strength, and a vulnerability to thermal cracking. The Current applications of ceramic matrix composites are in metal-cutting tools and chemically corrosive environments as well as areas in which the operating conditions involve elevated temperatures [11].

2.1.2 Polymer matrix composites (PMC).

The most common composites known as FRP - Fiber Reinforced Polymers (or Plastics). These materials use a polymer-based resin as the matrix, and a variety of synthetic fibers such as glass, carbon, aramid and natural fibers as the reinforcement. Matrix materials are either thermosetting or thermoplastic polymers. Reinforcing fibers are either continuous or chopped. The technology of polymer composites has been driven to a large extent by aerospace and military applications [11].

2.1.3 Metal matrix composite (MMC).

Metal matrices are usually ductile metal alloys of Aluminum, Magnesium, Titanium or Copper. Some of their relative advantages over polymer matrices include elevated operating temperatures, no inflammability and greater resistance to degradation by organic fluids but they are much more expensive than polymer matrices and possess high strength-to-weight ratio [11]. Depend on core materials it can be classified into three types they are:

i. **Metal matrix natural polymer composites:**

Hybrid composite materials built up from interlacing layers of thin metals and natural fibers core. Natural fibers can be obtained from plant, animal and mineral resources can be used as reinforcements in the manufacturing of green composite in the same way as the synthetic fibers but it can be low-temperature operation and low formability compared to metal matrix thermoplastic polymer composites

ii. **Metal thermosetting fiber reinforced polymer**:

Fiber metal laminates are hybrid composite materials built up from interlacing layers of thin metals and fiber reinforced adhesives. The metal currently being used is either aluminum, magnesium or titanium, and the fiber-reinforced layer is either glass fiber, carbon fiber, and aramid fiber reinforced composite. They exhibit very good weight-specific stiffness and strength properties. The main problem with these products is their predominant brittleness so that they are strongly limited by their deformation processes.

iii. **Metal thermoplastic polymer**.

Hybrid composite materials built up from interlacing layers of thin metals and thermoplastic adhesives materials have good formability for different sheet forming processes. Regardless of the variations, however, aluminum thermoplastic polymer composites offer the advantage of low cost over most other MMCs. In addition, they offer excellent thermal conductivity, high shear strength, excellent abrasion resistance,

high-temperature operation, no flammability, minimal attack by fuels and solvents, and the ability to be formed and treated on conventional equipment.

2.2 Adhesion

Adhesion performance has major priority in sandwich composites. In fact, if the material is not able to maintain proper adhesion between the different layers, the detached layers are no longer acting as a unique component. Hence the sandwich composite loses its mechanical performance. For this reason, the main requirement for sandwich composites is sufficient adhesive bonding between the three layers.

2.2.1 Adhesion mechanisms

Adhesion is a very complex and multi-disciplinary topic; in fact, it includes chemistry, thermodynamics, and mechanics. For this reason, the adhesion phenomenon is explained through many theories, between these: adsorption theory, mechanical interlocking model, electronic or electrostatic theory, weak boundary layer theory, diffusion or inter-diffusion theory, chemical bonding theory is the most adopted ones [12].

2.2.2 Adhesion in MPM sandwich composites

In adhesive bonding and especially in metal/polymer interfaces the failure modes are driven by the existing forces between adhesives and metal adherends. Those forces can be then divided into adhesive forces and cohesive forces. The former takes place at the interface metal/polymer, whereas the latter act between the polymer molecules of the adhesive itself or within the metal substrate. Figure 2.3 shows a schematic representation of the concepts just explained. It is clear to understand that the overall bonding strength depends on the balance between the two acting forces. If the adhesive forces are weaker than the cohesive ones (or vice versa), the failure always occurs at the lower load [13].

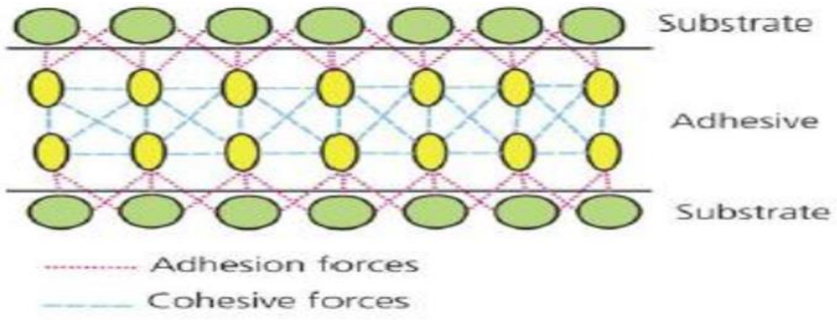

Figure 2. 3 :Schematic representation of adhesion and cohesive forces acting in adhesive bonds[20].

2.3. Mechanical Properties of MPM Sandwich Composites

The characterization of composites for mechanical properties is very important from design and analysis as well as life prediction point of view [14].

The literature work cited refers mainly to conventional sandwich composites with thick polymer cores. The simple structure of sandwich composites allows manufacturers to choose the aluminum alloy to be used as skin by looking at the mechanical properties required. The tensile test is one of the main evaluation methods used to characterize and specify the mechanical and forming potential of materials [5]. Obviously, changing the metal alloy, the properties of the material change significantly. Stiffer sandwich composites can be obtained at the cost of formability; consequently, designers have to match the characteristics of the material by taking into account the relative requirements.

2.4 Literature review of modern composite materials

Modern composite materials began in 1937 when salesmen from the Owens Corning Fiberglass Company began to sell fiberglass to interested parties around the United States [15].

Staut-Scarab is claimed to be the first car to use composites materials in the body structure, more precise glass fiber reinforced plastic (GFRP). The car was developed in 1945 for a small series and was designed by William Stout in cooperation with Owens Corning, who also developed the GFRP body panels and chassis [15].

In East Germany 1950 automotive industries began to use structural body parts from composite materials**.** Since those early days, it has been demonstrated that composites are lightweight, fatigue resistant and easily moulded to shape, a seemingly attractive alternative to metals [16].

GM and Kaiser Willys [15], Launched car models with GFRP semi-structural body parts, such as the Chevrolet Corvette shown in Figure 2. 4 and the Kaiser Darrin. The Corvette has after that continued to use glass fiber composite body panels and today it also uses carbon fiber material system in more structural parts.

Figure 2. 4 : Corvette body structure parts [21].

The Corvette was initially made from 46 composite part assembled by adhesive bonding. The assembly was initially challenging as the pieces were hand made with low accuracy which led to a labour intensive post-treatment of sanding and filling gaps.

In Japan 1970 most innovative manufacturers of automotive industries began use of structural composite materials from Aluminum/thermoplastic /Aluminum composite materials. By the early 1980 were also available in Germany and the U.S. From then on, adoption grew exponentially as architects, fabricators, and building discovered the functional advantages and beautiful possibilities of new materials such as; lightweight and impressive strength-to-weight ratio, material adaptability, and flexibility, durability, harmony with the environment and variety of colours [17].

In 1991 the Aluminum/polyethylene /Aluminum materials facility for automotive application began production, setting a standard for innovation and quality that

M. H. Parsa [18], Studied on strain state the sandwich sheet has higher formability in comparison to the aluminum sheet. Stabilizing effect that allows the material to deform in a quasi-stable manner, thereby delaying the onset of localized necking and increasing the forming limit in sandwich sheets. Contrary to as the experimental result of uniaxial tension of sandwich sheets show, deformation of the materials depends on the volume fraction of polymer core that has lower strain hardening exponent than monolithic aluminum face sheet. Thereby the lower FLD of monolithic aluminum-related to lower strain rate sensitivity factor and lower initial defect factor that compensated by higher strain hardening exponent.

Mohamed Harhash [19], Studied on SPS sandwich laminates can substitute the commercial sheets due to the improved thermal, acoustic damping and specific mechanical properties by investigated deep-drawable steel skin sheets and the polypropylene-polyethylene copolymer core layer.

H.P Mohamed [20], Studied on SPS formability is investigated through deep drawing and stretching. The deep drawing working area is determined at varied blank holding forces and draw ratios. The results revealed, that maximum drawing ratio decreases with thicker core layers and becomes more limited with thinner skin sheets as predicted by the mechanical properties. The stretching behavior of the SPS laminates is investigated using a semi-spherical punch. The stretching behavior of the SPS is negatively affected by increasing the core thickness.

Deniz Hara [21], Studied on replacement of sheet metal body panels with panels made from sandwich materials to decrease the mass of the car body thus contribute to improving motor emissions (due to reduced power needs thus smaller size motors when body weight is reduced). In the sandwich material configurations to achieve the target of decreasing the mass of body panels are investigated using finite element based simulations for static and vibrational behavior. Considering these benefits of sandwich

structures, they can be very widely used in car body design. The laminated metals with very thin viscoelastic core layers are mostly used for vibration dissipation.

Jianguang Liu [22], Studied on the bending deformation of the sandwich sheet can be divided into six portions: elastic tensile region and elastic compressive region in polymer core, an elastic tensile region in an outer metallic sheet, an elastic-plastic tensile region in an outer metallic sheet, and elastic-plastic compressive region in the inner metallic sheet. Due to the small deformation degree of core polymer and that the strain at the elastic limit of the polymer is much larger than that for the metal, the elastic deformation behavior with no viscous effect is considered for the core polymer. The elastic region of polymer follows Hooke's law and the stress in the transverse direction can be express. During the bending process, the skin sheet may undergo elastic, elastic-plastic, or full plastic deformations. It depends on the thickness of the core polymer and the yield stress of the aluminum alloy sheet. When the sandwich sheet is very thin and the bending radius is relatively large, the skin sheet undergoes elastic deformation and the bending angle will completely recover after unloading. For this case, the spring back angle does not need to be calculated. When the sandwich sheet is very thick and the bending radius is relatively small, the skin sheet will partially or completely undergo plastic deformation and then the bending angle will partially recover after unloading.

Abdolvahed Kami [23], Analyse SEM during the deformation of the SPS sheet, the fracture of the viscoelastic core layer occurs after the fracture of the metallic skin.

V. Harms [24], Analysis of crash structures consisting of MPM sandwich structures with a thermoplastic core exhibit a sufficient energy absorbing effectiveness, comparable or even better than metallic crash absorbers.

Changsoon Jang [25], Studied on lightweight materials have been sporadically used to substitute vehicle components and civil construction, but their vast utilization is limited by their reduced mechanical properties compared with standard materials, as in case of the comparison between steel and aluminum. However, the target of weight reduction can also be achieved by developing different typologies of materials, designed for specific applications. This is the case of a hybrid structure realized by

combining metals and polymers, the latter one which may be both reinforced or not. Much effort has been spent in the direction of characterizing the material properties, as well as in defining the possible industrial applications, of metal-polymer hybrid structures.

Luca Quagliato [26], Studied on SPS experiments described the typology of made of steel skin and sheet molding compound core have been utilized whereas three different adhesives, Being the adhesive of key importance for the cohesion of the laminate structure, three different types of epoxy-based resin have been tested, namely: N.F.W. Sealer, EP5055 and ABRO epoxy. From the results of the shear strength test, the adhesives which have good yield strengths have been utilized for the manufacture. Based on the results of the fracture surface, the best adhesion is represented by the EP5055 epoxy, whose shear strength has higher than the adhesion between the sheet molding compound core layers, as proved by the portion of sheet molding compound core remaining on the joining surface, on the steel part.

2.5 Gap of research work

MPM sandwich laminates used for different application due to has high formability, deep drawing, stretching, thermal insulator, high strength, energy absorption, impact force resist, light weights and so on. In the literature, several authors focused on the formability of metal-polymer laminate structure, no work in the direction of mechanical and physical properties of sandwich laminates with experimental setup and ANSYS Workbench simulation.

Hence the gap of previous research can be filling by manufacturing and experimental set up of physical and mechanical properties of AA6061/HDPE/AA606 sandwiches. These methods are used to determine the strength and lightweight of sandwich laminates.

Finally, to analysis the results that are agreements between experimental result and ANSYS Workbench simulation; which indicates that the rule of the mixture.

Chapter 3

Materials, methods and experimental setup

3.1 Materials

In this work materials are Aluminum alloy, HDPE and Epoxy resin with its hardener.

3.1.1 Aluminum alloy

Aluminum has excellent corrosion resistance and electrical conductivity. It is easily formed or cast and a very large number of commercial alloys are available. There are a vast number of applications, ranging from packaging (e.g. beverage cans, household foil) to whole aircraft structures. Architectural uses are very widespread. Vehicle manufacturers, increasingly conscious of weight, are moving towards maximizing aluminum-based engines and whole body structures. Depending on manufacturing process it can be classified two types [27]. which are;

a) **Casting Alloys:**

Manufacture by specific casting methods; e.g. sand, permanent mold, die-casting. The alloy composition and casting method affect the final metal structure. Some may be modified by subsequent heat-treatments to improve properties.

b) **Wrought Alloys:**

Shaped by plastic deformation (hot and/or cold working). For the purpose of comparison an aluminum alloy 6061 will be used, it is one of the more common and widely used alloys. The number 6061 represents the mixture of the alloy, contains magnesium and silicon as major elements. Commonly used for the purpose of high strength, good toughness, heat resistance, corrosion resistance and easy to work for welding [28].

3.1.2 High-density Polyethylene (HDPE)

Polyethylene is thermoplastic material which has low strength, hardness and rigidity. But has a high ductility and impact strength as well as low friction used for core materials. It can be classified depends on the principle of physical property density. The

differences in density are basically due to differences in the degree of crystallinity, which also influences the plastics' melting point ranges [16, 17]. Polyethylene plastics have the generally advantageous properties of toughness, high tensile strength, and good barrier properties to moisture.

3.1.3 Epoxy resin and its hardener

Epoxy adhesives consist of an epoxy resin plus a hardener. They allow great versatility in formulation since there are many resins and many different hardeners. Epoxy adhesives can be used to join most materials. Epoxies have good strength, do not produce volatiles during curing and have low shrinkage. However, they can have low peel strength and flexibility and are brittle. Epoxy adhesives are available in one-part, two-part and film form and produce extremely strong durable bonds with most materials [31]. Any resin system for use in a composite material will require the following properties:

- Good mechanical properties
- Good adhesive properties
- Good toughness properties
- Good resistance to environmental degradation

3.2 Material model and fundamental laws of behavior

Whilst deformation of homogeneous, isotropic materials can be described relatively simply by use of Young's and Shear moduli, which are bulk properties of the raw material. Simple properties of composite materials can be estimated based on the contribution of each part of the composite. This method is referred to as the rule of mixtures (RoM) [32].

The laminate structure composed of three different components, (AA6061) aluminum skins, HDPE core sheet and two thin adhesive layers between the aluminum skin and HDPE core, in order to enhance the cohesion of the structure.

Five different layers can be identified according to the figure 3.1, each one of them with an own stiffness and resistance cross-section. If the load is applied along the normal

direction of the cross-section of the laminate, all the plies will withstand the same elongation, hence the strain results in $\varepsilon_{Al} = \varepsilon_{PE} = \varepsilon_{AD}$, while the stress shall be different, according to the cross-section of each layer. When the laminate MPM material undergoes elastic deformations, its stiffness will be a combination of cross-sections area and Young's modulus of its components, namely of the stiffness of aluminum, adhesive and polyethylene layers [33].

Figure 3. 1:Schematic of the layup of the AA6061/HDPE/AA6061

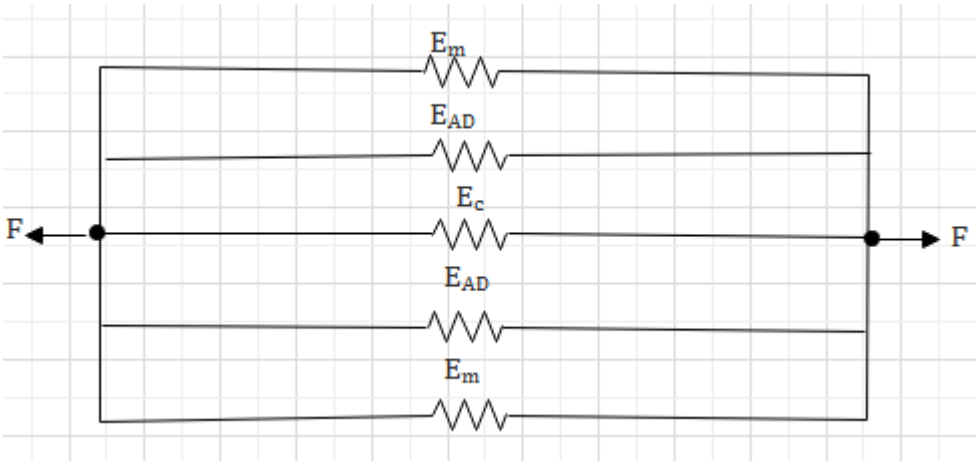

Figure 3. 2: Equivalent stiffness of the AA6061/HDPE/AA6061 sandwiches

The rule of mixtures refers to equivalent stiffness from the figure 3.2 shows that; Mathematical model of mechanical properties in terms of the bulk or mechanical properties relative amounts of its constituent phases for negligible resin Epoxy due to small thickness which shown from equation (3.1).

$$V_m + V_f = 1 \qquad (3.1)$$

Where, $V_f =$ volume fraction of the core

$V_m =$ volume fraction of the matrix

$$P_{sw} = P_m V_m + P_f V_f = P_m(1 - V_f) + P_f \qquad (3.2)$$

$$\sigma_{sw} = \sigma_m V_m + \sigma_f V_f \tag{3. 3}$$

Where, P_{sw} = Axial load is applied in the longitudinal direction of sandwich laminate

σ_{sw} =Yield stress longitudinal direction of sandwich laminate

This law was tested and stated for describing the properties of fiber-reinforced composites with an acceptable degree of accuracy [33]. However, the mixture rule for the sandwich materials has referred to the presence of negligibly small transverse stresses compared to axial or longitudinal stresses. The same law of mixtures can be modified to describe as shown equation (3.4) Young's modulus for the composite by assuming a uniform axial strain for the whole sandwich composite.

$$E_{sw} = V_m E_{m+} V_c E_c$$

$$\sigma_{y\ sw} = V_m \sigma_{y_m} + V_f \sigma_{y_c}$$

$$\sigma_{u\ sw} = V_m \sigma_{u_m} + V_f \sigma_{u_c}$$

$$\mathrm{V_{12}} = -\frac{\varepsilon_2}{\varepsilon_1} = \mathrm{V_f V_f} + \mathrm{V_m V_m} \tag{3.4}$$

$$\sigma_{f\ sw} = V_m \sigma_{f_m} + V_f \sigma_{f_c}$$

$$\rho_{sw} = v_m \rho_m + v_f \rho_c$$

$$G_{sw} = \mathrm{V_f G_c} + \mathrm{V_m G_m}$$

Homogenized material properties of sandwich laminates can be found by using properties of the aluminum alloy and HDPE and volumetric contribution. In table 3.1, the material property of AA6061 and HDPE are given. This material property is taken from [34] ,[28].

Table 3. 1:Material property of AA6061 and HDPE

	AA6061	HDPE
Density Kg/m^3	2700	952
Specific Heat Constant Pressure mJ/kgC^0	8.75^5	2.3^6

Young's Modulus (MPa)	68900	1100
Poisson's Ratio	0.33	0.42
Bulk Modulus(MPa)	69608	2291.7
Shear Modulus (MPa)	26692	387.32
Compressive Yield Strength (MPa)	280	0
Tensile Yield Strength(MPa)	280	25
Tensile Ultimate Strength(MPa)	310	33
Fracture strain elongation	0.17%	0.3%
Offset yielding elongation	0.02%	0.02%
Ultimate strain elongation	0.04%	0.04%
Melting point range, °C	650	120-130

Homogenized material properties of sandwich laminates can be depending on Dimensional parameters. Table 3.2 can be expressed mathematical model of material on different dimensional for fundamental law behavior of longitudinal direction sandwich laminates on different thickness.

Table 3. 2 : Mathematical model of material property.

A_m = cross sectional area of the skin $= 2(t_m * w_m) = 300mm^2$	t_m = thickness of the skin=0.5mm w_m = widness of the skin = 300mm
A_c = cross sectional area of the core $= t_c * w_c = 450mm^2$	t_c = thickness of the core = 1.5mm w_c = widness of the core=300mm l_m = Length = 300mm
V_m = volume fraction of the matrix = $\frac{2\text{Volume of matrix}}{\text{volume of sandwich}} = 0.4$	V_{ms} = volume of the skin=$t_m * w_m * l_m = 45{,}000mm^3$ V_c = volume of the core = $t_c * w_c * l_s = 135{,}000mm^3$

$V_f =$ volume fraction of the core $= \frac{\text{Volume of core}}{\text{volume of sandwich}} = 0.6$	$V_{sw} =$ volume of the sandwich $= 2V_{ms} + V_c = 225{,}000mm^3$ $A_{sw} =$ area of the sandwich $= 2A_m + A_c = 750mm^2$

The resulting properties of a composite material can also be described by the concept of interaction between different properties of the material. In table 3.3 can be summarized on fundamental behavior of longitudinal sandwich laminates from equation (3.4). However, the mixture rule for the sandwich materials has referred to the presence of negligibly small transverse stresses compared to axial or longitudinal stresses.

Table 3. 3 : summaries on mathematical model properties of MPM sandwich laminates

	MPM laminates		
	AA6061/PE/6061	AA6061/PE/6061	AA6061/PE/6061
t_c=Thickness of the core mm	1.5	2	2.5
t_m=Thickness of the skin mm	0.5	0.5	0.5
Total thickness	2.5	3	3.5
V_f= Volume fraction of the core	0.6	0.67	0.7143
V_m=Volume fraction of the matrix	0.5	0.33	0.2857
Density Kg/m^3	1,651.2	1,528.84	1,451.4
Young's Modulus (MPa)	28,220	23,473	20,470
Poisson's Ratio	0.384	0.3904	0.3943
Shear Modulus (MPa)	10,909	9,067.8	7,902.5
Tensile Yield Strength(MPa)	127	109.5	97.85
Tensile Ultimate Strength (MPa)	143.8	124.45	112.14

3.3 Manufacturing of AA6061/HDPE/AA6061 Sandwich Sheets

The AA6061/HDPE/AA6061 sandwich sheets were fabricated by manual spindle pressing machine. The mold was prepared 300x300x4mm dimensional and a pre-heated 180^0c in the furnace. Manually laminated resin epoxy was inserted between the AA6061 skin and HDPE in the 180^0c hot die. During the process, a constant force of 160kN has been applied, both top and bottom die which have been kept at the constant temperature of 180°C for 7–10 min as shown in Figure 3.3. Three kinds of sandwich sheets with core thicknesses of 1.5, 2 and 2.5 mm were prepared to investigate the influence of the thickness ratio on the strength of the sandwich sheet.

Figure 3. 3 : a) manual spindle pressing machine b) Three kinds of sandwich sheet products

3.4 Experimental procedure and setups

3.4.1 Specimen sampling procedure

The test used in this research required to cut each laminate into smaller pieces. For various experiments which are the different thickness of specimen prepared by EN 323 standard and (ASTM D3039) specimen geometries.

a) For density and hardness test specimen

b) For tensile test specimen

Figure 3. 4 : sandwich sheets cut in to small pieces

3.4.2 Specimens Geometry and Dimensions

The specimen geometry of experimental test and ANSYS simulation were conducted according to by EN 323 standard and (ASTM D3039) within the dimension of AA606/HDPE/AA6061 sandwich sheets as shown figure 3.5 [14].

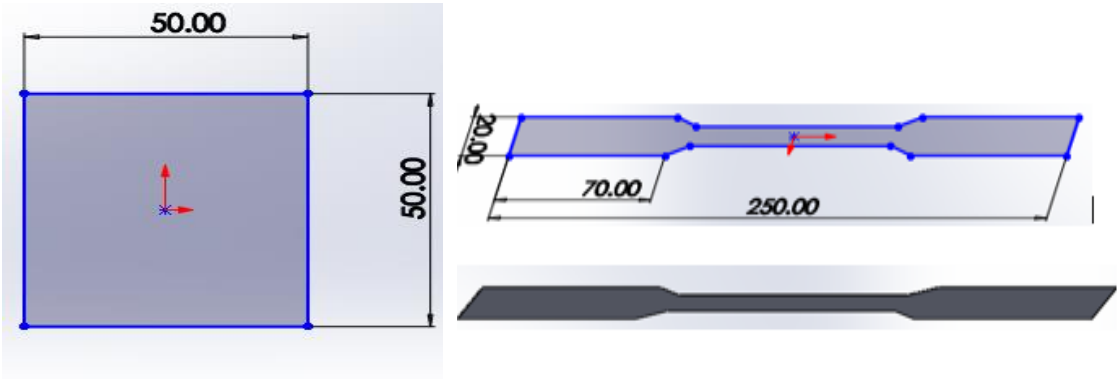

a) Density and hardness test specimen b) Tensile test specimen

Figure 3. 5:Test specimen dimensions

3.4.3 **Specimen testing procedures**

After the AA6061/HDPE/AA6061 sandwich sheet, composite Specimens cut into the desired dimension the tests were follow according to standard dimension of sandwich sheets; such as density, hardness and tensile test for each set of the specimen.

3.5 Density test of MPM sandwich laminates

Determination of MPM density was done following EN 323 standard. Test samples were cut in squares, with a side length of 50 x 50 mm. The thickness of the conditioned test samples were measured to an accuracy of 0.01 mm for the width and length using sliding digital Vernier caliper [35]. The weights of the test samples were recorded using a precise digital weighting balance shown as figure 3.5 for different thickness sandwich sheets.

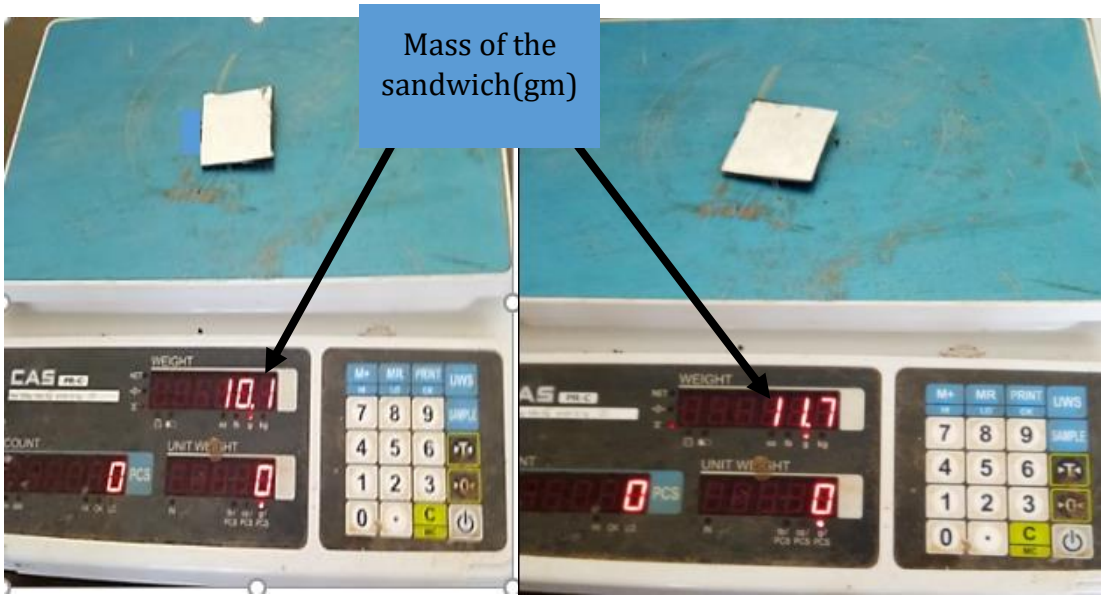

a) 2.5mm sandwich sheet b) 3mm sandwich sheet

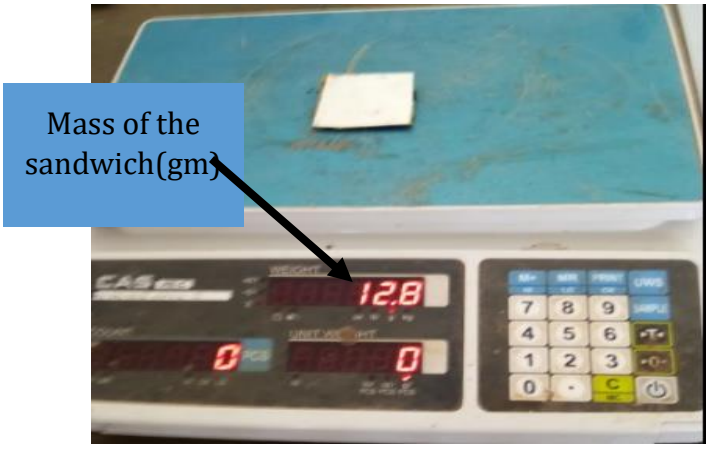

c) 3.5mm sandwich sheet

Figure 3. 6 : Precise digital weighting balance MPM sandwich sheets.

From figure 3.6 the recording mass weight of sandwich sheets can be analysis density of MPM sandwich sheets using the following equation (3.5);

$$\rho = \frac{M}{V} \tag{3.5}$$

Where: ρ: Density of a test sample, in kg/m3

M: Mass of a test sample, in kg

V: Volume of a test sample, in m^3 = Length*Width*Thickness

3.6 Hardness test of MPM sandwich laminates

Hardness has a variety of meanings. To the metals industry, it may be thought of as resistance to permanent deformation. To the metallurgist, it means resistance to penetration. Which has a collection of different methods for measuring a definite characteristic of metallic materials, namely:

- The resistance to penetration of a specific Indenter (defined by fixed form and properties),
- Under the application of a certain static force
- For a definite time,
- Using precise measuring procedures.

Determination of hardness testing was done the following ASTM E 140, Standard hardness conversion tables for metals. Hardness conversion values for other metals based on comparative test on similar materials having similar mechanical properties will be added to this standard as the need arises [36]. Rockwell Hardness is probably the most used hardness testing method because it is simple and self-contained, so that there is no need for a separate microscope reading. The type of Rockwell hardness (the Scale) defined by a letter establishes the indenter and the loads applied, The Rockwell hardness test samples were recorded by using standard force (150kgf) shown as figure 3.7 for different thickness sandwich sheets. [37].

a) 2.5mm sandwich sheet b) 3mm sandwich sheet

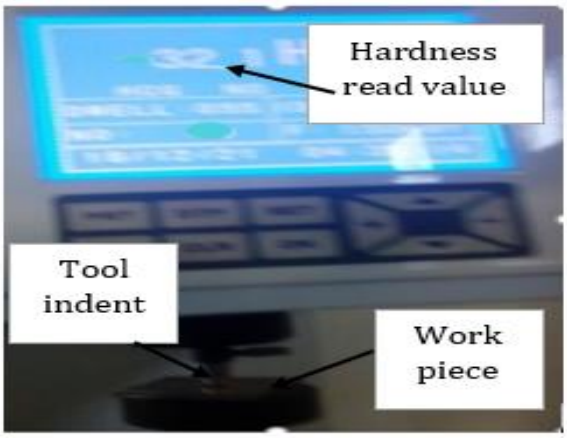

c) 3.5mm sandwich sheet

Figure 3. 7 : Rockwell hardness contact recording

3.7 Introduction of mechanical properties the test apparatus

UTM Testing Systems are highly integrated testing packages that can be configured to meet different testing needs. Each includes a load unit with the integrally mounted actuator and servo valves, a hydraulic power unit, and the control system. The control system has three major parts: the system software running on a personal computer, the digital controller, and a remote station control panel. These functions work together to provide fully automated test control. Optional application software packages let you further tailor the system to automate most any standard or custom test procedure.

3.7.1 Tensile strength test (ASTM D3039/D3039M)

Experimental setup tensile properties, such as tensile strength, tensile modulus, and Poisson's ratio of flat composite laminates, are determined by static tension tests in accordance with ASTM D3039 [14].For each sample, 3 specimens were tested to get approximation results with ANSYS Workbench simulations. The dimension of specimen was 250x20x2.5, 250x20x3, 250x20x3.5mm depending on HDPE thickness respectively. During the test the specimens were placed in the grips of UTM and axial load is applied through both the ends of the specimen. Typical points of interest when testing a material include: ultimate tensile strength (UTS) or peak stress; The cross-head speed used was 0.5 mm/min, and gauge length was 200 mm. Load-elongation curve, breaking load, peak stress and % strain at peak stress were acquired in real time by machine and provided at the end of each test. Typical specimen under tensile strength test is shown in figure 3.8.

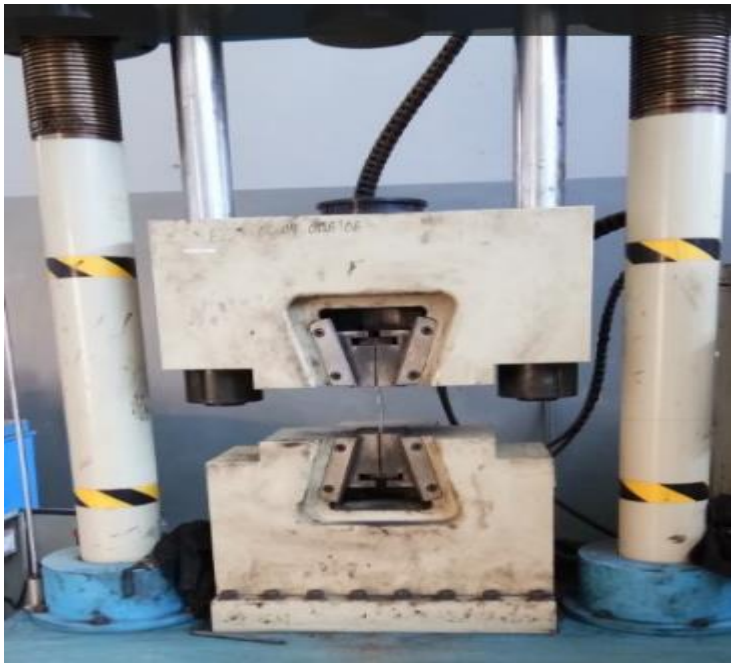

a) Before breaking tensile test

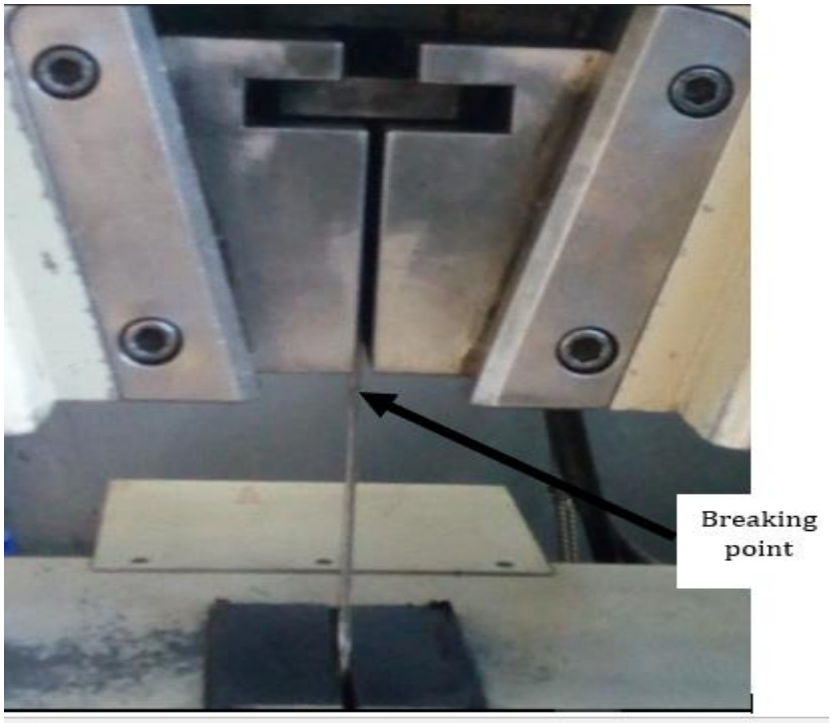

b) After breaking tensile test

Figure 3. 8 : Typical specimen under tensile strength test

Chapter 4

Finite element modeling and analysis of MPM sandwich laminates

There are many software packages available used to analysis composite materials. Such as LS-DYNA, ABAQUS, SOLID work, MSC NASTRAN, ANSYS WORK BENCH and so on. Those software are used to analysis the result of materials for a particular application, before the actual structures are constructed. The important of prediction of MPM sandwich laminates for constructions are to know mechanical properties and cohesive zone model by ANSYS Workbench analysis.

4.1 Modeling of mechanical property and finite element analysis

Modeling of mechanical property materials is a preliminary condition in the design and fabrication process of structural parts in order to obtain stiffness and strength under varying loading conditions [14]. To understand the behavior of the composite materials under different loading conditions used to determine the ability of application composite materials. Studying the mechanical properties becomes vital. The result is used for the selection of material for a particular application before the actual structures are constructed. Such as mechanical properties of sandwich laminates are three-point bending, tensile strength, and impact force analysis under static load conditions.

4.2 Finite element modeling and analysis of three-point bending sandwich sheets

Three-point bending properties of sandwiches were determined according to ASTM C393 with midspan point loading configurations [38]. In a first step load was applied by means of steel bars, in order to determine sandwich bending stiffness and shear rigidity; which are defined as a materials ability to resist deformation under load performed on the composites samples to evaluate the value of inter-laminar shear strength (ILSS).: A typical simply supported sandwich panel consists of two thin faces with a thickness of $\boldsymbol{t_f}$, separated by a light and a weaker core of the thickness $\boldsymbol{t_c}$, as illustrated in Equation (4.1) [39]. The overall depth of the panel is d and the width b.

The faces are typically bonded to the core which is to provide a load transfer mechanism between the main components of the sandwich panel. The flexural rigidity for a sandwich beam, denoted as D, is the sum of the flexural rigidities of the faces and the core measured with respect to the centroid axis of the entire section and can be expressed as:

$$\text{Flexural stiffness } D = \frac{E_f b \boldsymbol{t_f}^3}{6} + \frac{E_f b \boldsymbol{t_f}\left[\boldsymbol{t_f}+\boldsymbol{t_c}\right]^2}{2} + \frac{E_c b \boldsymbol{t_c}^3}{12}$$

$$\text{Bending strength } \sigma_b = \frac{3F_{max}L}{2bd^2}$$

$$\text{Bending Modulus } E_b = \frac{FL^3}{4bd^3D}$$

$$\text{Facing strength } \sigma_f = \frac{F_{max}L}{2b\boldsymbol{t_f}(d-\boldsymbol{t_c})} \qquad (4.1)$$

$$\text{Core shear stress } \tau_{cmax} = \frac{F_{max}}{2bd}$$

$$\text{Core shear stiffness } \boldsymbol{Q} = \frac{\boldsymbol{G_c}\left(\boldsymbol{d}-\boldsymbol{t_f}\right)^2}{\boldsymbol{t_c}}$$

Where; b: Width of specimen [mm]

d: Total thickness of sample [mm]

D: Deflection due to a force F in bending [mm]

F: Force [N]

F_{max}: Maximum force during compression/bending [N]

L: Support span length [mm]

$\boldsymbol{t_f}$: Facing thickness [mm]

$\boldsymbol{t_c}$: Core thickness [mm]

σ_b: Bending strength[Mpa]

E_f: Young's modulus of the face sheet[Gpa]

E_c: Young's modulus of the core sheet[Gpa]

4.2.1 Mathematical integration of Finite Element Analysis

Three-point bending was typically implemented in finite element codes as to analysis elasticity of bending modulus and shear force between the plains. The equation of mathematical model 2D FEM can be expressed according to equation (4.2)

The internal work done by the virtual strain (δε) in the domain (Ω) and potential energy of distributed load force general displacement (**ψ**) surface tractions in the domain (S) are equal to the external concentration force applied on virtual displacement (d) as neglected weight of the body force, it follows;

$$\frac{1}{2}\int_{\Omega}\{\varepsilon\}^T\{\sigma\}d\Omega - \int_S\{\psi\}^T\{T\}\,dS = \{d\}^T\{P\} \tag{4.2}$$

where T is the traction surface and P is the external force applied. The (2D) modeling Four-node isoparametric elements were used to model the sandwich beam, with the element dimensions continuously decreasing towards the loading and stress concentration points [40]. Which are defined standard shape functions of isoparametric elements as shown equation (4.5), i.e.

$$\frac{1}{2}\int_{\Omega}\{d\}^T\{B\}^T\{D\}\{B\}\{d\}d\Omega - \int_S\{d\}^T\{N\}^T\{T\}dS = \{d\}^T\{P\} \tag{4.3}$$

where N is matrices of shape functions for bulk and cohesive elements, B is the derivative of N; d are nodal displacements, v are passion ratios and D is the material tangential stiffness matrix for the bulk elements.

$$\text{For plane stress}\begin{Bmatrix}\sigma_x\\ \sigma_y\\ \tau_{xy}\end{Bmatrix} = \frac{E}{1-v^2}\begin{bmatrix}1 & v & 0\\ v & 1 & 0\\ 0 & 0 & \frac{1-v}{2}\end{bmatrix}\begin{Bmatrix}\varepsilon_x\\ \varepsilon_y\\ \gamma_{xy}\end{Bmatrix} \qquad D = \frac{E}{1-v^2}\begin{bmatrix}1 & v & 0\\ v & 1 & 0\\ 0 & 0 & \frac{1-v}{2}\end{bmatrix} \tag{4.4}$$

$$(\boldsymbol{\psi})=\begin{Bmatrix}U(x,y)\\ V(x,y)\end{Bmatrix}=\begin{bmatrix}N_1 & 0 & N_2 & 0 & N_3 & 0 & N_4 & 0\\ 0 & N_1 & 0 & N_2 & 0 & N_3 & 0 & N_4\end{bmatrix}\begin{Bmatrix}U_1\\ V_1\\ U_2\\ V_2\\ U_3\\ V_3\\ U_4\\ V_4\end{Bmatrix} =\{N\}\{d\} \tag{4.5}$$

4.2.2 Specimens geometry and boundary conditions

The specimen geometry of three-point bending dimension was conducted according to the (ASTM C393) to analysis ANSYS Workbench simulation with mathematical model analysis. The Standard dimension of geometry 3-point bending has expressed according to the following figure 4.1 with parameters properties of material taken from table 3.1.

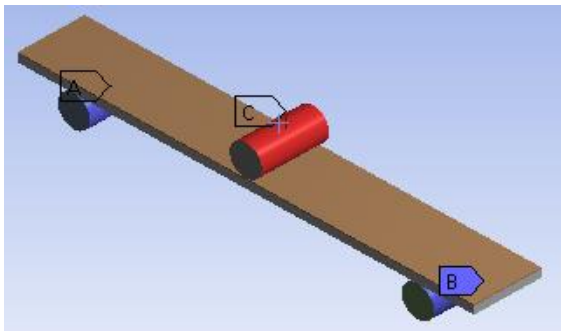

LAC: 64mm

LCB:64

b: 25mm

t : 2.5mm

A: Fixed support

B: Fixed support

C: 250N force applied

Figure 4. 1: Geometric modeling and boundary condition of three point bending.

4..2.3 Meshing specimen geometry

The geometry is developed by solid work and imported into static structural ANSYS Workbench. The appropriate element size is selected according to the geometry features to discrete elements and meshing by 4 mm within 14211 nodal elements as expressed according to the following figure 4.2

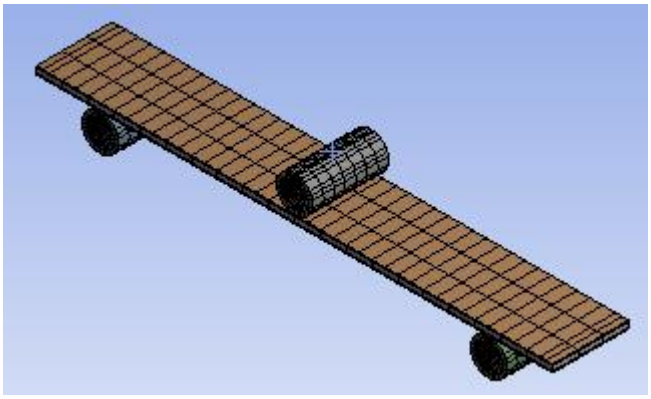

Figure 4. 2: Discrete and mesh into nodal elements

4.3 Finite element modeling and analysis of tensile Strength Sandwich Sheets

The tensile ANSYS Workbench simulation is one of the main evaluation methods used to characterize and specify the mechanical and forming potential of materials. Material properties like Young's modulus, yield stress, strain hardening coefficient and the true stress Vs true strain curve are the basic input parameter required for the pre-processing different application [41]. The modeling standard of tensile simulation is determined by static tension ANSYS Workbench simulation in accordance with ASTM D3039 [14].

4.3.1 Specimens geometry and boundary conditions

The specimen geometry of tensile simulation dimension was conducted according to the **(**ASTM D3039) to analysis ANSYS Workbench simulation with mathematical model analysis. The Standard dimension of geometry tensile simulation has expressed according to the following figure 4.3 with parameters properties of material taken from table 3.1.

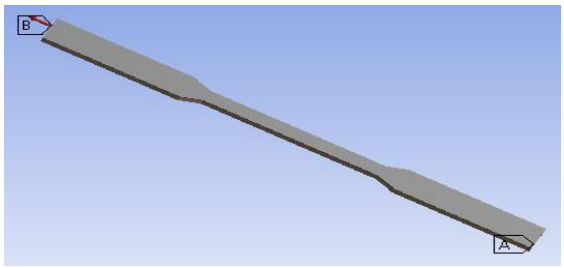

LAB: 250mm

t : 2.5mm

b: 20mm

A: Fixed support

B: 2.8Kn force applied

Figure 4. 3 :Geometric modeling and boundary condition of tensile strength.

4.3.2 Meshing specimen geometry

The geometry is developed by solid work and imported into static structural ANSYS Workbench. The appropriate element size is selected according to the geometry features to discrete elements and meshing by 4 mm within 1292 nodal elements as expressed with the following figure 4.4

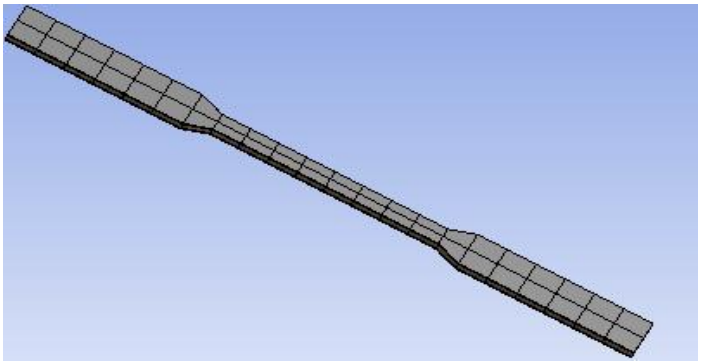

Figure 4. 4 : Discrete and mesh into nodal elements.

4.4 Finite element modeling and analysis of impact force sandwich sheets

The impact properties of a material represent its capacity to absorb and dissipate energies under impact or shock loading. A variety of standard impact test methods are available for metals (ASTME23) and unreinforced polymers (ASTM D256) [42]. Basically low and high-velocity simulation should be performed to understand the dynamic loading effect on the MPM. The modeling of low-velocity impact ANSYS Workbench simulation was carried out using a drop weight impact tower with free fall is known the weight and diameter hemispherical nose can define as equation (4.6) this equation can analysis the maximum impact load increased up to a threshold value while the energy absorption of the structure increased with increasing impact energy.

$$Total\ energy = Potential\ energy + Kenetic\ energy$$

$$\frac{1}{2}\sigma A\varepsilon L = mg(h + \varepsilon L)$$

$$\frac{1}{2}\frac{F}{A}A\varepsilon L = mg(d + \varepsilon L) \qquad (4.6)$$

$$F = \frac{2mg}{\varepsilon L}(d + 1)$$

Where; σ: Yield stress(Mpa)

m: impactor mass[Kg]

h: height of drop impactor[m]

g: standard earth gravity[m/s^2]

ε : Maximum elastic strain[mm/mm]

L: length [m]

A: area[m^2]

F: Maximum impact force resistance [N]

4.4.1 Energy balance model (Theory)

After we solve the static contact problem we apply the methods to the problem of the low-velocity impact of functionally graded sandwich panels. Solving the static contact problem first and combining the solution with the dynamic response of the sandwich panel obtained via simple spring-mass models (quasi-static assumption) accomplish this. The use of static load-deflection behavior of the sandwich beam in the impact analysis needs some justification. In general, the wave propagation effects, especially through the thickness of the core, should be considered in impact response of sandwich panels [43]. The impact response of the sandwich structures was modeled using a theoretical approach, based on the energy-balance model in order to examine the relative effects of the bending, shear and indentation components of the deformation. The sandwich beam was modeled as a combination of two springs Figure 4.5, according to the model proposed by Shiva Kumar et al. [13]: a linear spring Kbs to account for the global deflection wb and a nonlinear spring Ki to represent the local indentation effects.

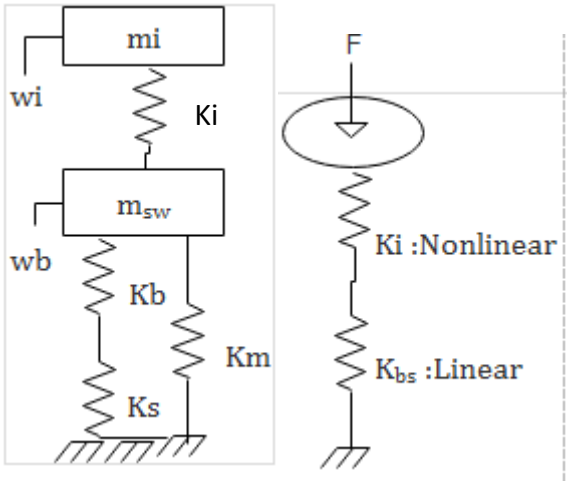

Figure 4. 5: Two DOF spring model for sandwich laminates

The springs are in series and represent the bending and shear effects neglecting the membrane effect due to nonlinearity. The global stiffness can be represented as

$$\frac{1}{K_{eq}} = \frac{1}{K_b} + \frac{1}{K_s} \tag{4.7}$$

$$K_{bs} = \frac{K_b * K_s}{K_b + K_s}$$

Using the numerical results from the contact problem we determined spring constants $K_i$and K_{bs} and the exponent n such that

$$F = K_i \alpha^n \tag{4.8}$$

$$F = K_{bs} w_b \tag{4.9}$$

Where ,$\alpha = w_b - w_i$

where F is the total load, α is the core indentation, w_b is the vertical displacement of the core at the at bottom face sheet interface.

The displacement of the impactor is calculated as the sum of indentation depth (core compression) and the global deflection of the sandwich beam:

$$w = w_b + \alpha = \frac{F}{K_{bs}} + \left(\frac{F}{K_i}\right)^{1/n} \tag{4.10}$$

The work done by the impactor during the impact event can be expressed as

$$W = \int_0^w F dw = Fw - \int_0^F w dF = Fw - \int_0^F \left(\frac{F}{K_{bs}} + \left(\frac{F}{K_i}\right)^{1/n}\right) dF$$
$$= \frac{F^2}{2K_{bs}} + \frac{n}{(n+1)} \frac{F^{1+n/n}}{K_i{}^{1/n}}$$

Considering that the impactor kinetic energy is equal to the work done or the strain energy stored in the springs, the maximum contact force can be calculated from

$$\frac{F_{max}{}^2}{2K_{bs}} + \frac{n}{(n+1)} \frac{F_{max}{}^{1+n/n}}{K_i{}^{1/n}} = E_b + E_s + E_C = \frac{m v_0{}^2}{2} \tag{4.11}$$

where m and v are the mass and the impact velocity of the impactor and the subscript b, s and c refer to energy dissipation in bending, shear and contact effects, respectively.

4.4.2 Specimens geometry and boundary conditions

The specimen geometry of impact force analysis dimension was conducted according to the (ASTME23) ANSYS Workbench simulation with mathematical model analysis. The Standard dimension of geometry impact force analysis has expressed according to the following figure 4.6 with parameters properties of material given from table 3.1.

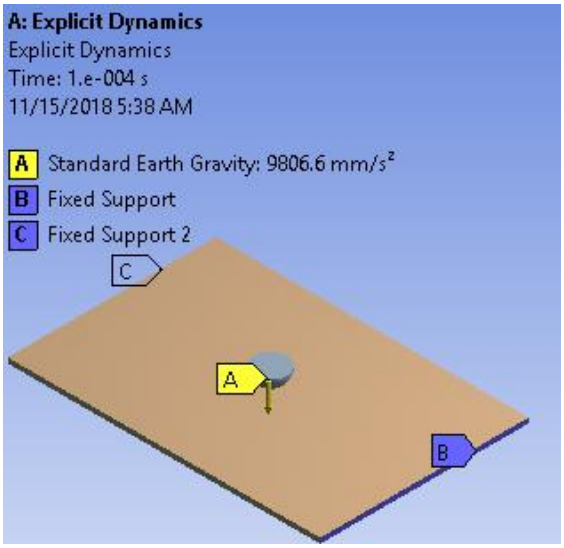

LCB:150mm

b : 100mm

t : 2.5mm

c: Fixed support

B: Fixed support

A: Standard earth gravity

Impactor rigid surface

Mass=2.5kg

Diameter =16mm

Velocity=25m/s

Figure 4. 6: Geometric modeling and boundary condition of impact force

4.4.3 Mesh specimen's geometry

The geometry is developed by solid work and imported into Dynamic Explicit ANSYS Workbench. The appropriate element size is selected according to the geometry features to discrete elements and meshing by 4 mm elements as expressed according to the following figure 4.7

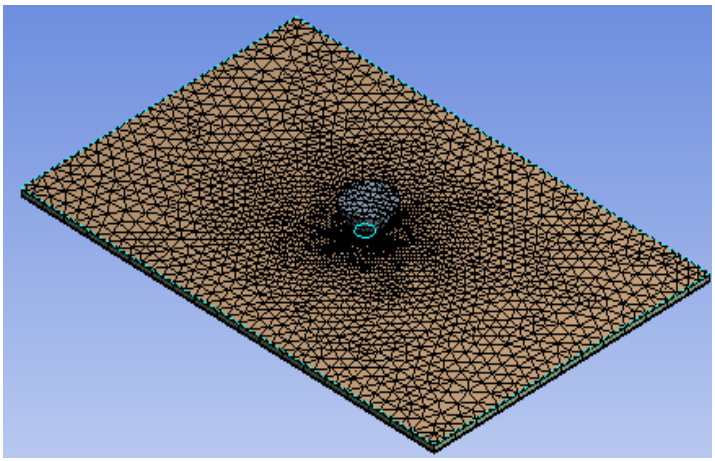

Figure 4. 7: Discrete and mesh into nodal elements

4.5 Cohesive zone model theory

The cohesive zone modeling (CZM) was used to simulate the interfacial adhesion condition between skin aluminum-alloy sheet and core polymer. In these adhesive structures, the performance of the adhesive interface layer is of crucial importance in providing effective stress transfer. However, damage may easily occur due to stress concentration or bond imperfection under loading. Thus, the mechanical properties of the adhesive interface layer are critical in the design and application of adhesive structural components in general engineering applications [44].

CZM can be used to model the delamination at interfaces directly in terms of traction versus separation using a traction-separation law. CZM assumes a linear elastic traction separation law prior to damage and assumes that failure of the cohesive bond is characterized by progressive degradation of the cohesive stiffness, which is driven by a damaging process. Damage is assumed to initiate when a quadratic interaction function involving the contact stress ratios (as defined in the expression below) reaches a value of one. This criterion can be represented as

$$\left\{\frac{t_n}{{t_n}^0}\right\}^2 + \left\{\frac{t_s}{{t_s}^0}\right\}^2 + \left\{\frac{t_t}{{t_t}^0}\right\}^2 = 1 \qquad (4.12)$$

where t_n, t_s and t_t refer to the stress in the normal, the first, and the second shear directions, respectively. ${t_n}^0$, ${t_s}^0$ and ${t_t}^0$ represent the peak values of the contact stress when the separation is either purely normal to the interface or purely in the first or the second shear direction, respectively.

4.5.1 Concepts of cohesive zone

Traditional linear elastic fracture mechanics solutions have stress singularity at the crack tip and it is difficult to measure the stress field very close to the crack tip. Cohesive zone eliminates the stress singularity and limits it to the cohesive strength of the material. This softening is simulated by a traction-separation law as shown in Figure 4.8. The traction-separation law is within a “cohesive zone” along the plane of potential crack propagation [45].

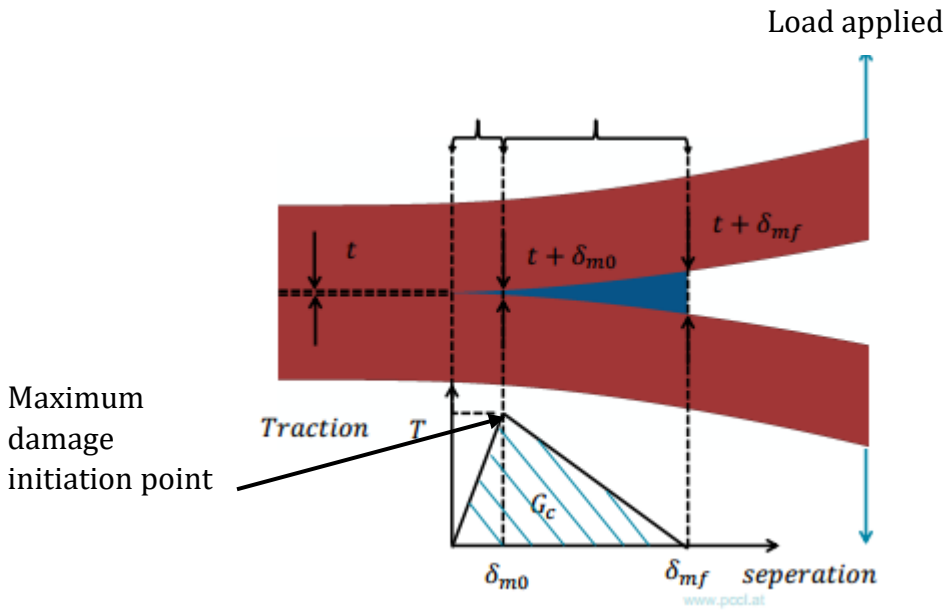

Figure 4. 8 : A cohesive zone damage evaluation and initiation [45].

The cohesive law is governed by a constitutive equation relating the traction across the interface with the interfacial separation. Crack initiation is related to the cohesive strength, i.e., the maximum traction on the traction-separation law. When the area under the traction-separation law reaches the fracture toughness, the traction declines to zero and new crack surfaces are generated [46]. This phenomenon is shown in Figure 4.9 traction-separation law.

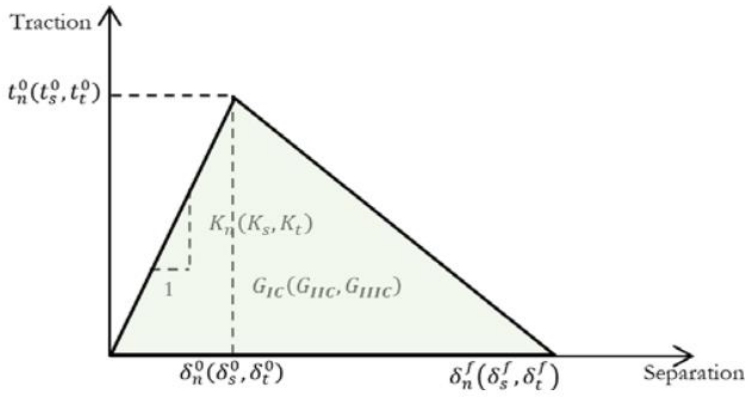

Figure 4. 9: Typical traction-separation response [46].

The available model in ANSYS Workbench assumes initially linear elastic response till interfacial strength, followed by damage initiation and evolution. The elastic behavior

is written in terms of an elastic constitutive matrix that relates the nominal stresses to the nominal strains across the interface. The default value of the original constitutive thickness is 1.0 if the traction-separation response is specified, which ensures that the nominal strain is equal to the separation (i.e. relative displacements of the top and bottom faces). The nominal strains can be defined as

$$\varepsilon_n = \frac{\delta_n}{T_0} \quad \varepsilon_s = \frac{\delta_s}{T_0} \qquad \varepsilon_t = \frac{\delta_t}{T_0} \tag{4.13}$$

where δ_n, δ_s and $\delta_t$are components of relative displacement between the top and bottom surfaces of the cohesive element, and T_0 is the original thickness of the cohesive element

4.5.2 Adhesive fracture energy

The total area under the curve of the traction-separation response is the critical fracture energy of the adhesive. It is a measure of the adhesive fracture toughness and is the amount of work needed to create a unit area of a fully developed crack [47]. It is a material constant and has a unit of N/m in the SI system.

4.5.3 Damage evolution

The initial response of the cohesive elements at each damage model is based on linear elastic fracture mechanics (LEFM) and is assumed to be linear until a crack initiation criterion is satisfied. The penalty stiffness, Ki, of each traction-separation response law that relates traction to the separation of cohesive elements before crack initiation is defined as below [46]:

$$K_i = \frac{\sigma_{ic}}{\delta_{ic}} \tag{4.14}$$

where i = I, II and III is fracture modes,σ_{ic} and,δ_{ic} are the cohesive strength and critical separation of pure modes of fracture, respectively.

The dependence of the fracture energy on the mode mix can be defined based on a power law fracture criterion. The power law criterion state that failure under mixed-mode conditions is governed by a power law interaction of the energies required to cause failure in the individual (normal and two shear) modes. It is given by

$$\left\{\frac{G_n}{{G_n}^C}\right\} + \left\{\frac{G_s}{{G_s}^C}\right\} + \left\{\frac{G_t}{{G_t}^C}\right\} = 1 \tag{4.15}$$

where G_n, G_s and G_t refer to the work done by the traction and its conjugate separation in the normal, the first, and the second shear directions respectively. ${G_n}^C$, ${G_s}^C$ and ${G_t}^C$ refer to the critical energies required to cause failure in the normal, the first and the second shear directions, respectively.

4.5.4 Numerical implementation

The implementation of the CZM in the finite element framework requires cohesive elements for modeling crack initiation, evolution and final failure and continuum elements for the surrounding bulk material. The cohesive elements are herein formulated exploiting the principle of virtual work [48]. The internal work done by the virtual strain (δε) in the domain (Ω) and the virtual crack opening displacement (δΔ) along the crack line (Σ_c) is equal to the external work done by the virtual displacement (δ**u**) at the traction boundary (Σ), it follows

$$\frac{1}{2}\int_{\Omega}\{\varepsilon\}^T\{\sigma\}d\Omega - \int_{\Sigma_c}\{\delta\Delta\}^T\{T\}\,d\Sigma_c = \int_{\Sigma}\{\delta u\}^T\{P\}\,d\Sigma \tag{4.16}$$

where T is the traction vector along the cohesive zone and P is the external traction vector. The crack face opening is interpolated to the Gauss integration points by means of standard shape functions, i.e.

$$\frac{1}{2}\int_{\Omega}\{d\}^T\{B\}^T\{D\}\{B\}\{d\}d\Omega - \int_{\Sigma_c}\{d\}^T\{N_c\}^T\{T\}\,d\Sigma_c = \int_{\Sigma}\{N\}^T\{P\}\,d\Sigma \tag{4.17}$$

where N and N_c are matrices of shape functions for bulk and cohesive elements, respectively; B is the derivative of N; d are nodal displacements , v are passion ratios and D is the material tangential stiffness matrix for the bulk elements.

$$\text{For plane stress } \begin{Bmatrix}\sigma_x\\ \sigma_y\\ \tau_{xy}\end{Bmatrix} = \frac{E}{1-v^2}\begin{bmatrix}1 & v & 0\\ v & 1 & 0\\ 0 & 0 & \frac{1-v}{2}\end{bmatrix}\begin{Bmatrix}\varepsilon_x\\ \varepsilon_y\\ \gamma_{xy}\end{Bmatrix} \qquad D = \frac{E}{1-v^2}\begin{bmatrix}1 & v & 0\\ v & 1 & 0\\ 0 & 0 & \frac{1-v}{2}\end{bmatrix} \tag{4.18}$$

The stiffness matrix and load vector of the cohesive elements are assembled in a user-defined subroutine within the commercial FE code Standard.

4.5.4 The finite element model theory

Cohesive zones are typically implemented in finite element codes as interface elements. Most (2D) cohesive zone models provide a constitutive relation between the normal opening displacement, normal traction and a separate relation between the tangential opening displacement and the tangential traction

4.5.5 Specimens geometry and dimensions

For the strength-based model and the cohesive model, an initial crack of small displacement opening by 10mm and fixed at one side to get the point of damage initiation. The AA6061 and HDPE sheets are considered isotropic. The material properties and cohesive law parameters are given in Table 4.1.

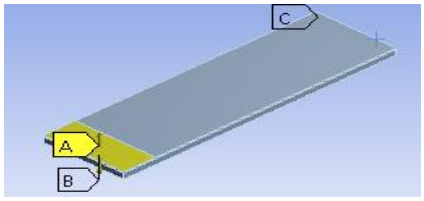

L: 75mm

b: 25mm

t: 2mm

a_0 : 10mm

A: 25mm Remote displacement

B :25mm Remote displacement

C: Fixed support

Figure 4. 10: Geometric modeling and boundary condition analysis of CZM

4.5.6 Strength-based fracture cohesive surface model

A linear interface cohesive element between AA6061 and HDPE sandwich sheets can be modeled equal thickness of cohesive elements. Therefore, the computed strains from the nodal forces can be equal to the displacements. The actual geometrical thickness of these elements in a FE Model is zero despite the fact they are solid elements. The sandwich sheet surfaces are defined using discrete rigid by 4mm elements since cohesive surface interaction requires a node to surface contact. A node set is created for the sheet surface consisting of initially bonded nodes.

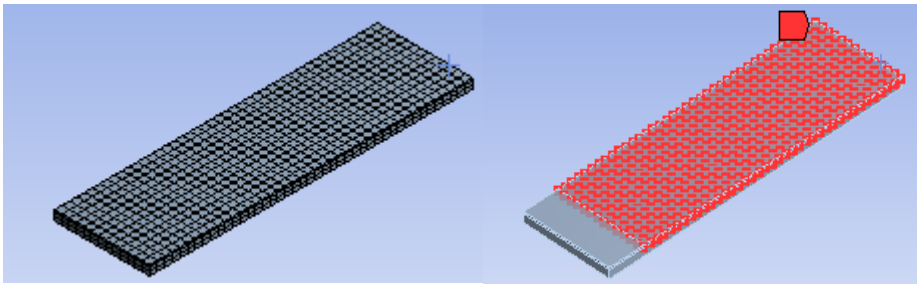

Figure 4. 11 : Meshing and interface delamination of sandwich sheets

Table 4. 1: Material parameters for the cohesive surface model [5].

Parameter	Symbol	Value	Units
AA6061 Elastic Modulus	E	68.9	Gpa
Poisson's ratio	V	0.33	
Polyethylene Elastic Modulus	E	1.1	Gpa
Poisson's ratio	V	0.42	
Cohesive thickness	t	0.05	mm
Peak contact stress	$t_n{}^o$	5.3	Mpa

Chapter 5

Results and discussion

5.1 Experimental and ANSYS Workbench simulation results

ANSYS Workbench simulation results are good reasonably agreements between the theoretical analysis and Experimental work, which indicates that the rule of the mixture.

5.1.1 Experimental density tests

Experimental density test of AA6061/HDPE/AA6061 to determine the density of sandwich sheets. These Results are compare with the experimental measured and rule of the mixtures as shown from table 5.1.

Table 5. 1 : weight balance to determine density results with theoretical analysis

Sandwich Thickness (mm)	Density test equation $\rho = \frac{M}{V}$			Theoretical equation $\rho_{sw} = v_m\rho_m + v_f\rho_c$
	Mass (gm)	Volume (mm^3)	Density (Kg/m3)	Density (Kg/m^3)
2.5	10.1	6250	1616	1651.2
3	11.7	7500	1560	1528.84
3.5	12.8	8750	1462	1451.4

$$\rho = \frac{M}{V} \quad (3.5)$$

Where: ρ: Density of a test sample, in kg/m3

M: Mass of a test sample, in kg

V: Volume of a test sample, in m^3

v_m: Volume fraction of the skin

v_c: Volume fraction of the core

ρ_m: Density of the skin

ρ_c: Density of the core

ρ_{sw}: Density of the sandwich

Density Vs thickness of three different AA6061/HDPE/AA6061 sandwich sheets are analysis on figure 5.1 within results taken from table 5.1.

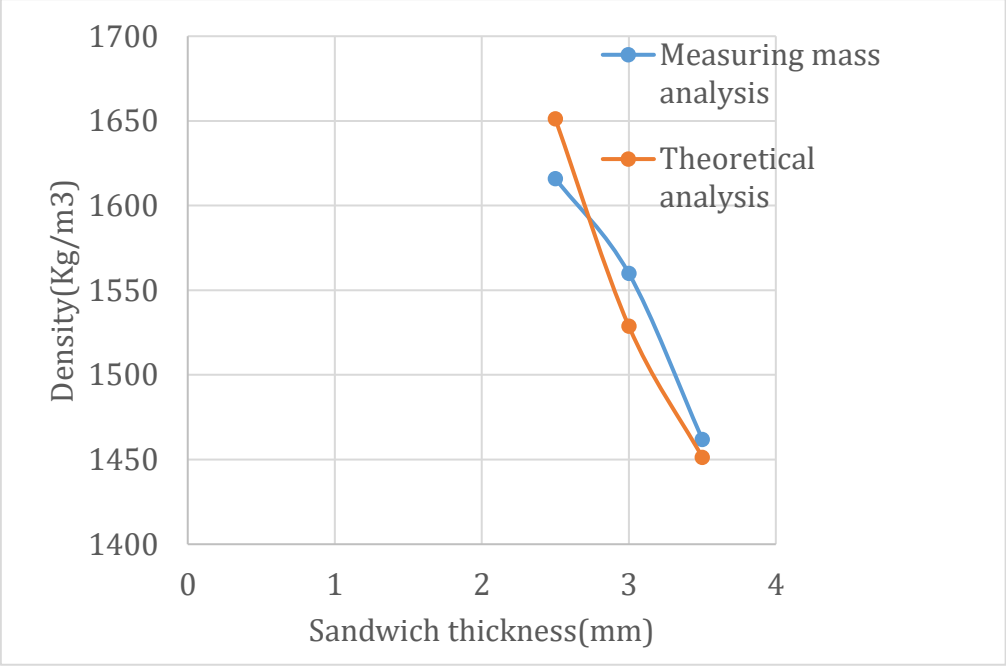

Figure 5. 1: Density Vs thickness of sandwich sheets

Shows from the figure 5.2 the density test specimen sandwich sheets determined by experimental tests and mathematical modeling rule of mixture. The density test specimen revealed that the density of sandwich sheets decreases with increasing the thickness of the HDPE layer. The results show that there are reasonably good agreements between the experimentally measured and rule of the mixtures values. Generally, the core thickness of sandwich laminates in order to design directly proportional with the lightweight of material, high strength to weight ratio, cost performance and pressure resist during the force applied.

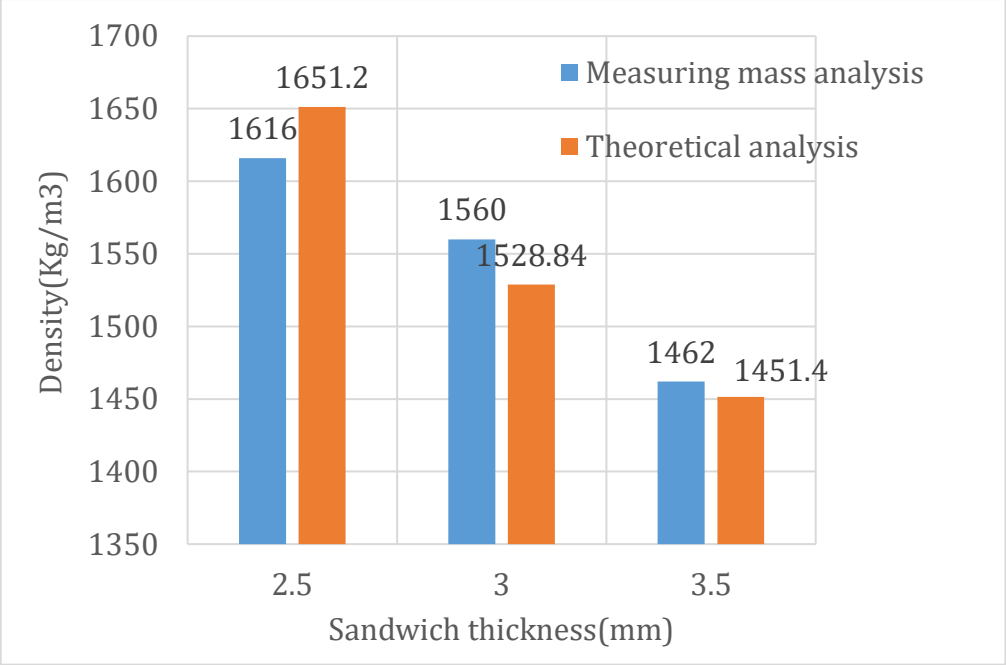

Figure 5. 2 : Density Vs thickness of sandwich sheets

5.1.2 Hardness test depth penetration of specimen results

Experimental hardness test of AA6061/HDPE/AA6061 to determine depth penetration of Rockwell hardness (C Scale) defined by a letter establishes the indenter and the load applied by using standard force (100kgf).

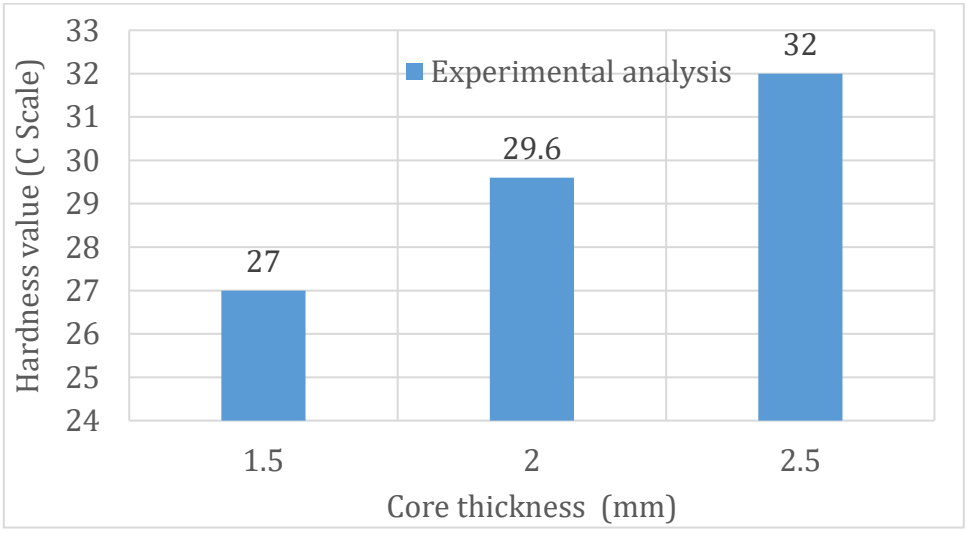

Figure 5. 3 : Experimental hardness Vs core thickness

MPM hardness stand for the ability to resistance to permanent deformation of material, energy absorption, impact force and vibration damping resistances. The hardness of AA6061/HDPE/AA6061 sandwich sheet is higher than that of the monolithic AA6061 sheet and it increases with increasing the thickness of HDPE core.

5.1.3 Experimental and ANSYS simulation tensile results

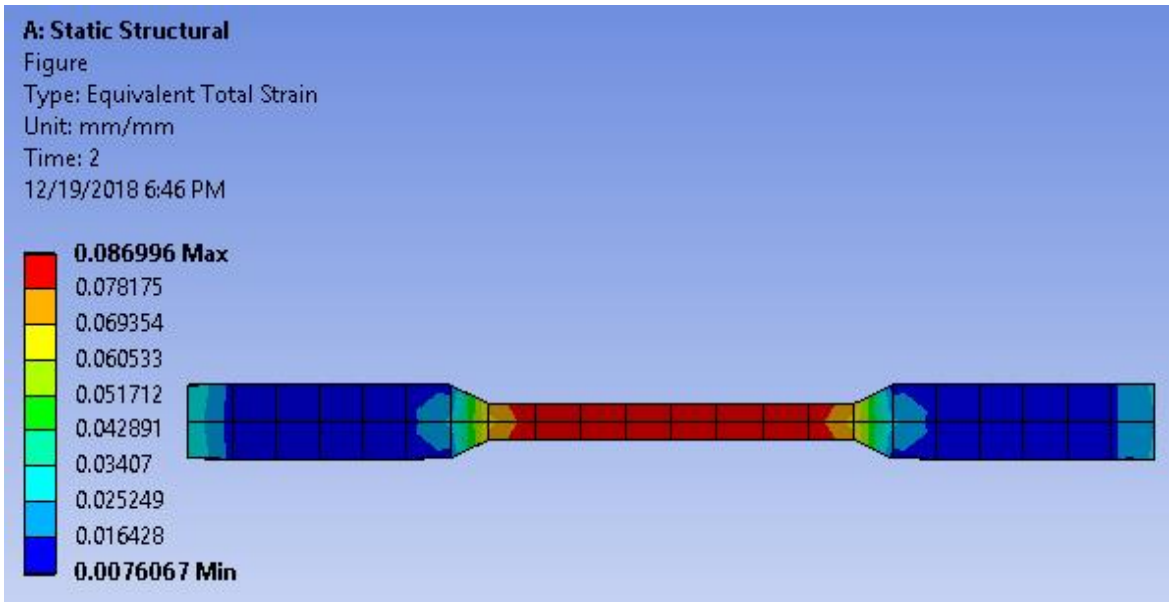

a) Thickness of 2.5mm sandwich sheet

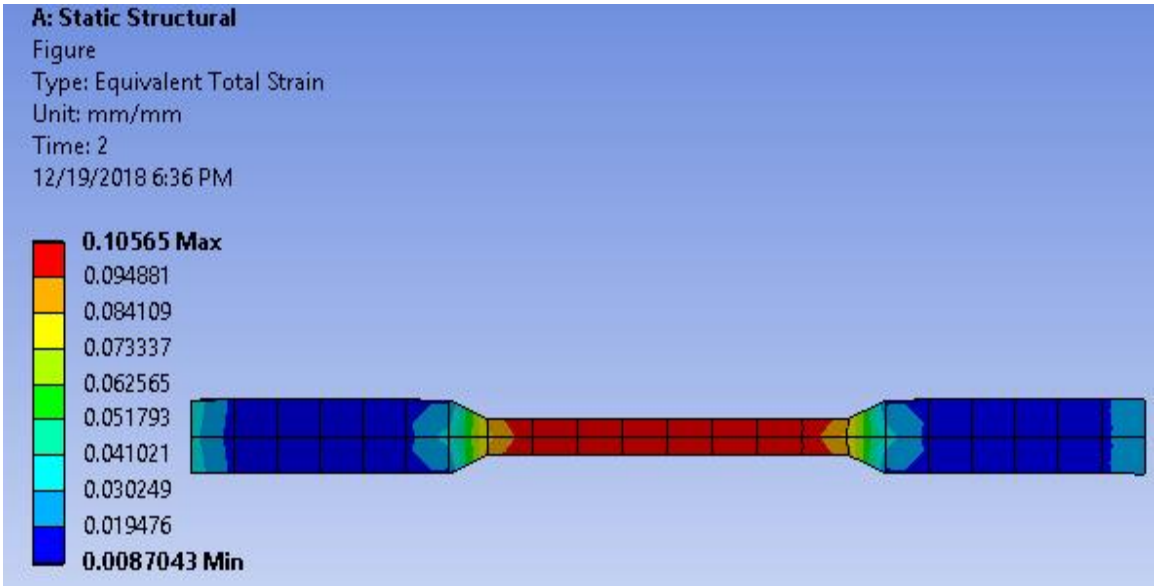

b) Thickness of 3mm sandwich sheet

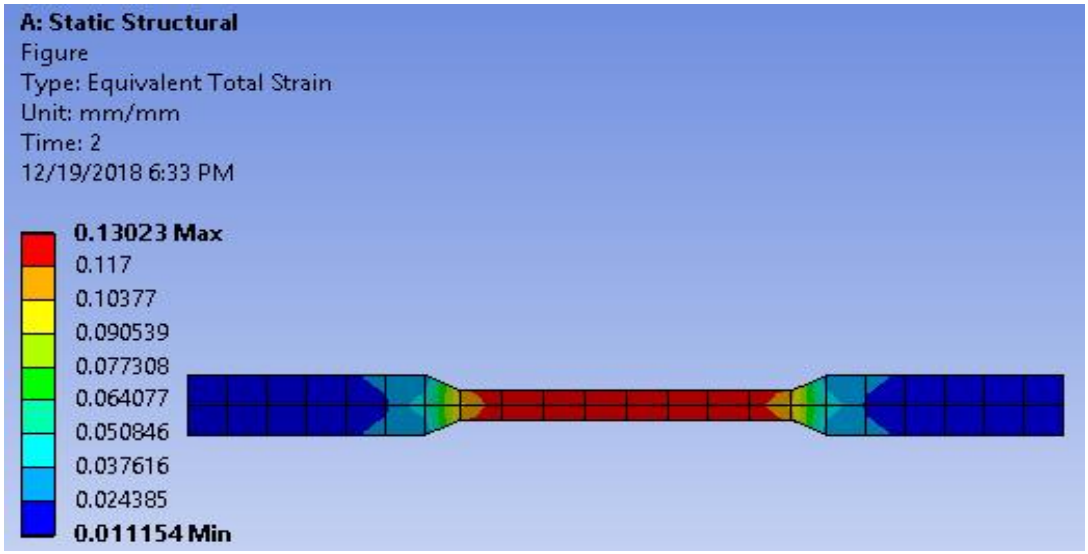

c) Thickness of 3.5mm sandwich sheet

Figure 5. 4 : Equivalent total strain for three thickness of sandwich laminates.

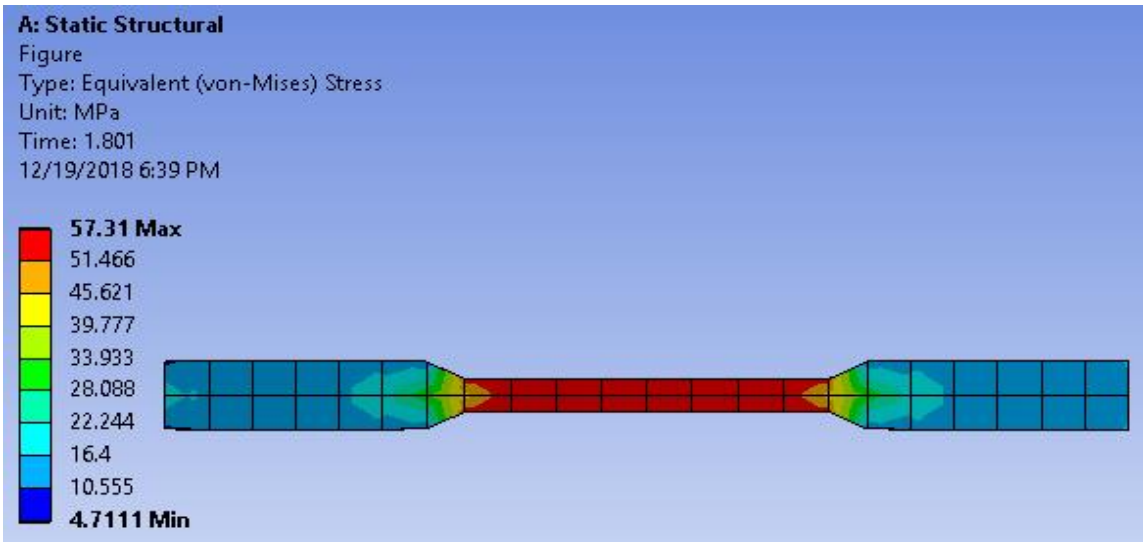

a) Thickness of 2.5mm sandwich sheet

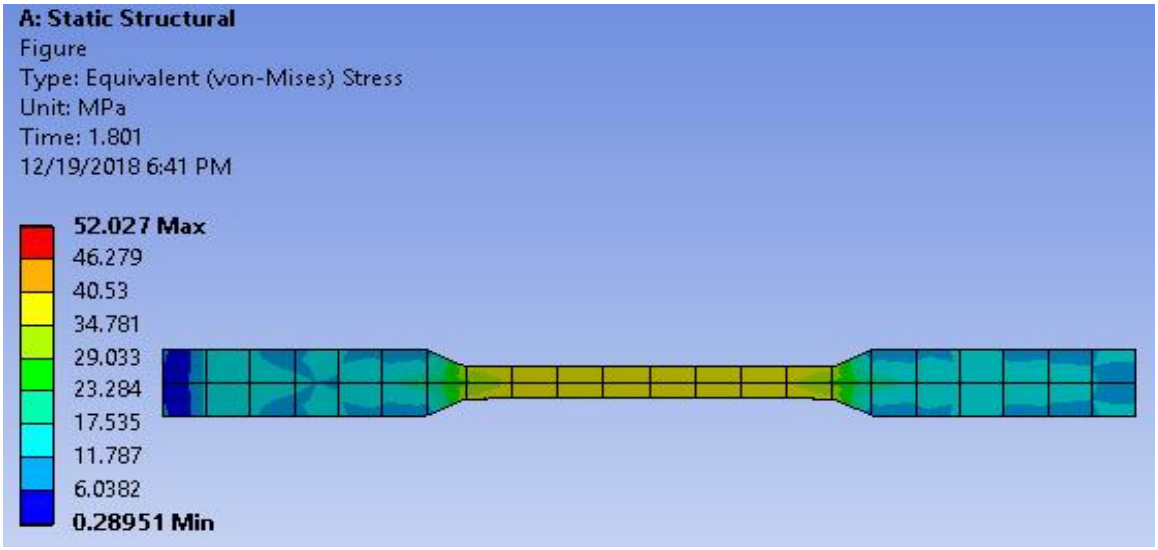

b) Thickness of 3mm sandwich sheet

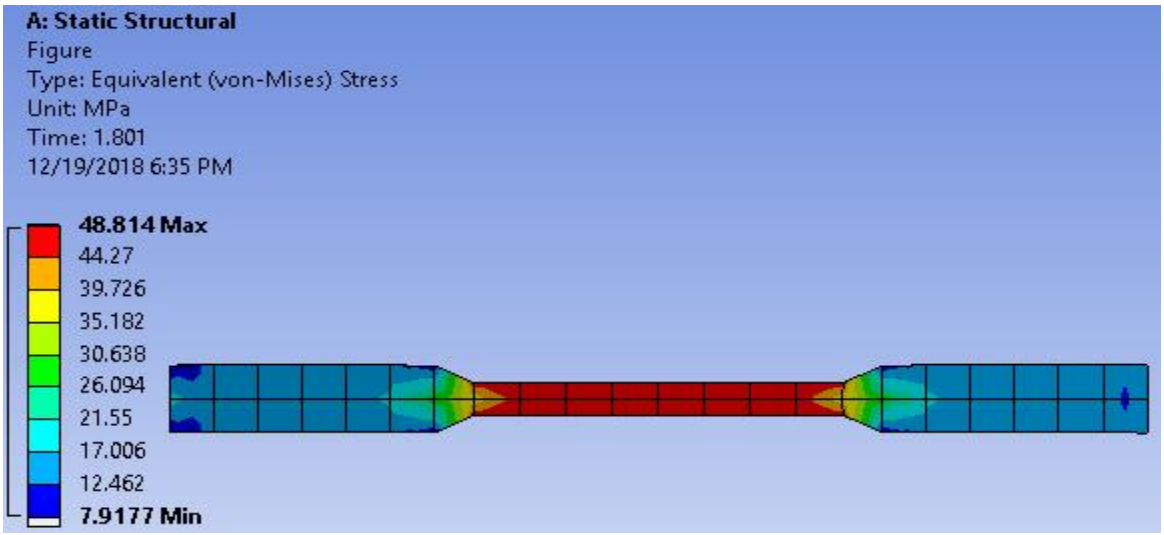

c) Thickness of 3.5mm sandwich sheet

Figure 5. 5 : Von Misses stress for three thickness of sandwich laminates.

stress Vs strain three different thickness of AA6061/HDPE/AA6061 sandwich sheets are analysis on figures 5.6 &5.7 within results taken from experiment test and ANSYS simulation shown on appendix table A1.

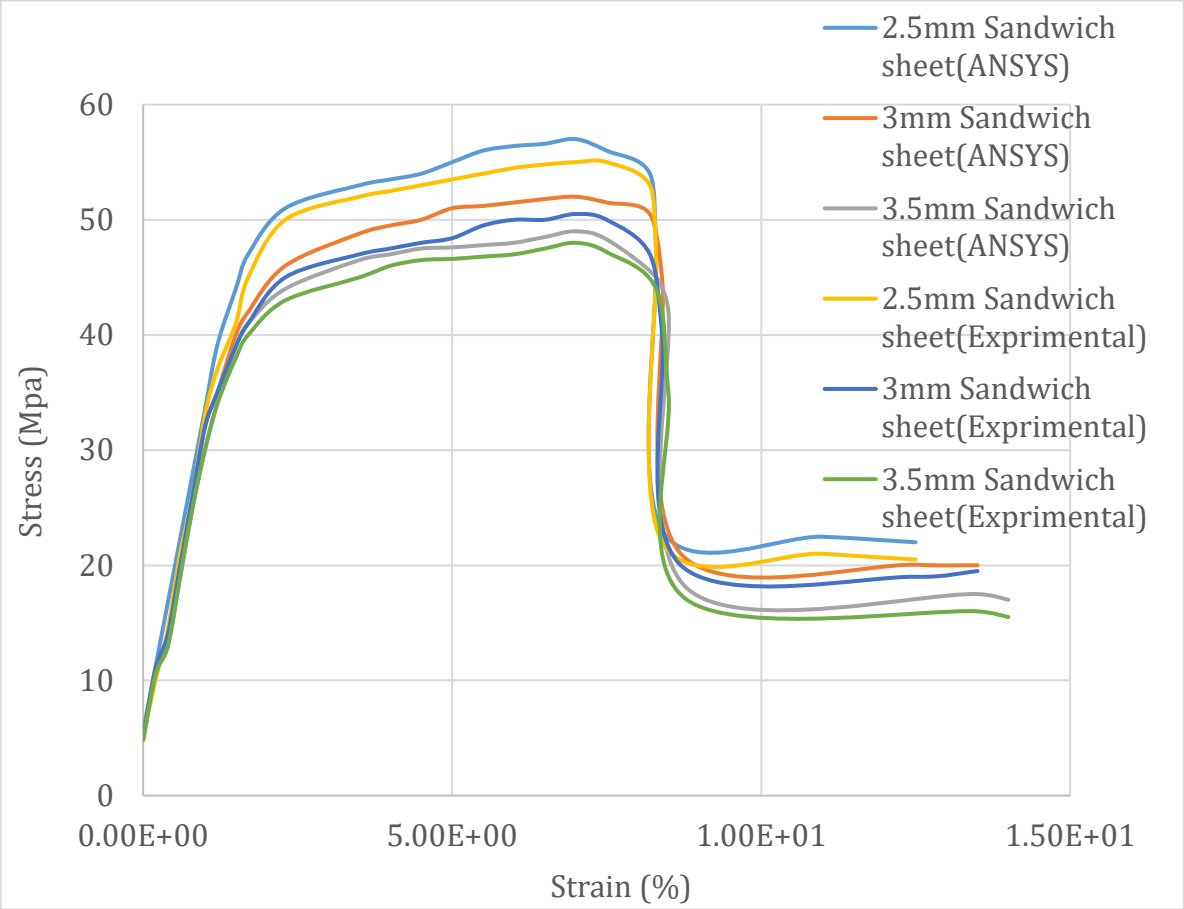

Figure 5. 6 : Experimental and Simulation plots for Stress Vs strain engineering

The engineering strain-nominal stress curves of sandwich sheets determined by tensile tests and ANSYS simulation with justify the rule of mixture. For analytical purposes, a plot of stress (σ) versus strain (ε) are constructed during tensile test experiment, which could be done automatically on the software provided by the instrument manufacturer. From the experiment, the value of stress unit (Mpa) is calculated by dividing the amount of force (F) applied by the machine in the axial direction by its cross-sectional area (A), which is measured prior to running the experiment. Mathematically, it is expressed in Equation 5.1.

The strain values, which have no units, can be calculated using Equation 5.2. In the equation, L is the instantaneous length of the specimen and L_o is the initial length.

$$\sigma = \frac{F}{A} \tag{5.1}$$

$$\varepsilon = \frac{L - L_o}{L_o} \tag{5.2}$$

Figure 5. 6.shows stress-strain curve is typical for ductile metallic elements. Once a material reaches its ultimate stress strength of the stress-strain curve, its cross-sectional area would reduce dramatically, a term known as necking. It shows that a stress-strain curve is divided into four regions, which are as follows: elastic, yielding, strain hardening (commonly occurs in metallic materials) and necking. The area under the curve represents the amount of energy needed to accomplish each of the "events." The total area under the curve (up to the point of fracture) is also known as the modulus of toughness.

The area under the linear region of the curve is known as the modulus of resilience. This represents the minimum amount of energy needed to deform the sample. The material will return to its original shape when a force is released while the material is in its elastic region. The slope of the curve, which could be calculated using Equation 5.3 is a constant, and is an intrinsic property of a material, is known as the elastic modulus, E. In metric unit, it is usually expressed in Pascal (Pa).

$$E = \frac{\sigma}{\varepsilon} \tag{5.3}$$

$$\text{Actual error (\%)} = \frac{\text{Exprimental results} - \text{ANSYs Workbench resuls}}{\text{Exprimental results}} \tag{5.4}$$

The actual error we get 12%,5% and 2.3% for 2.5mm,3mm and 3.5mm sandwich sheets respectively which are obtained from equation 5.4

Generally, the results show that there are reasonably good agreements between the experimentally measured and ANSYS simulation values, which indicates that the rule of the mixture. From Figure 5.7 shows that the elongation of AA6061/HDPE/AA6061 sandwich sheets is directly proportional to the thickness core and inversely proportional to the tensile stress of sandwich composite materials.

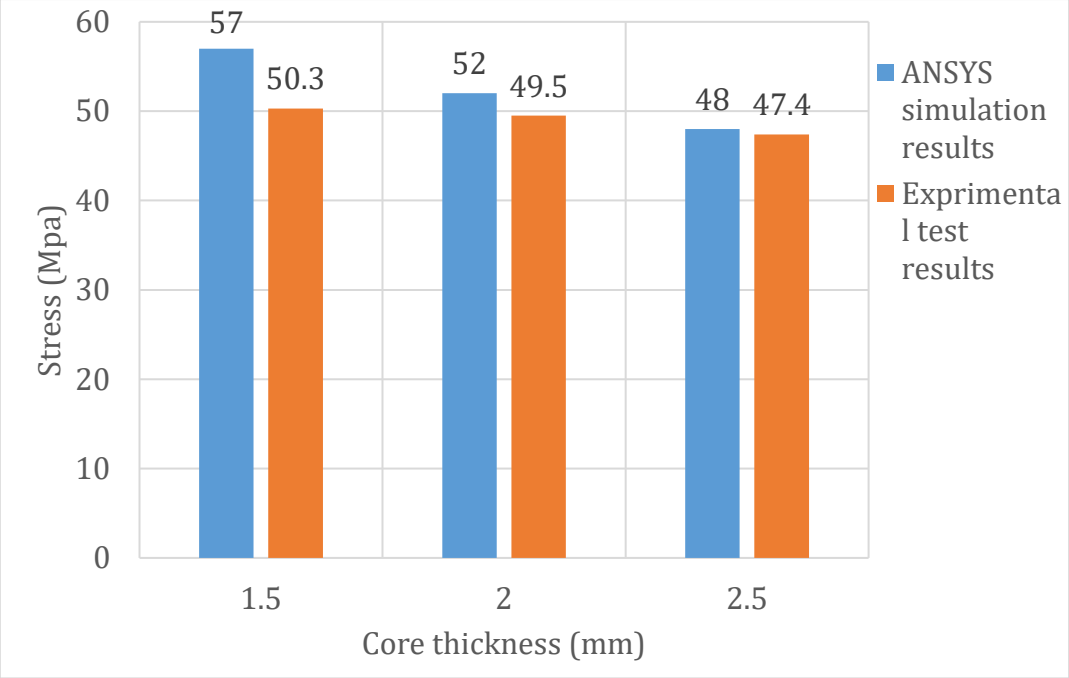

Figure 5. 7 : Maximum stress values Vs thickness of sandwich sheets

5.1.4 Three-point bending simulation results

The three-point bending results are analysis under static load by ANSYS workbench. such as; total deformation, equivalent stress and strain energy as shown below figures.

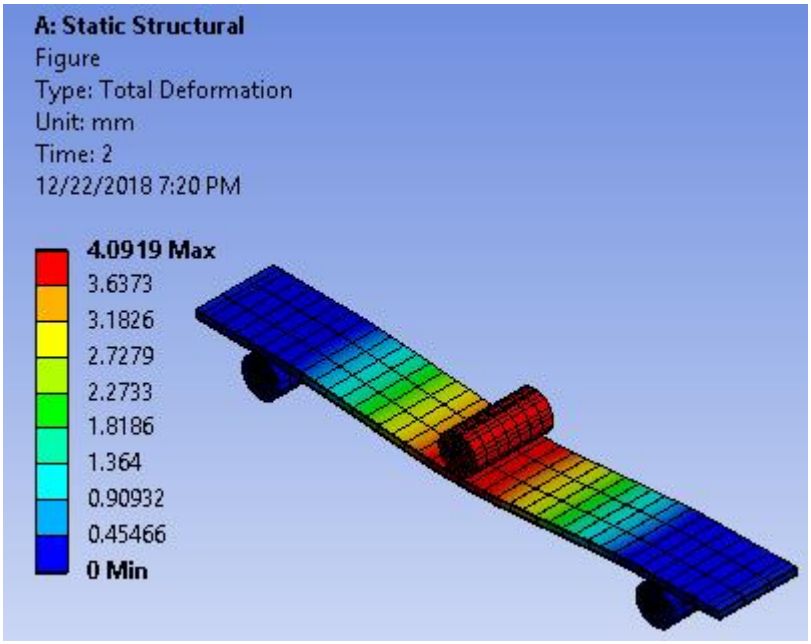

a) Thickness of 2.5mm sandwich sheet

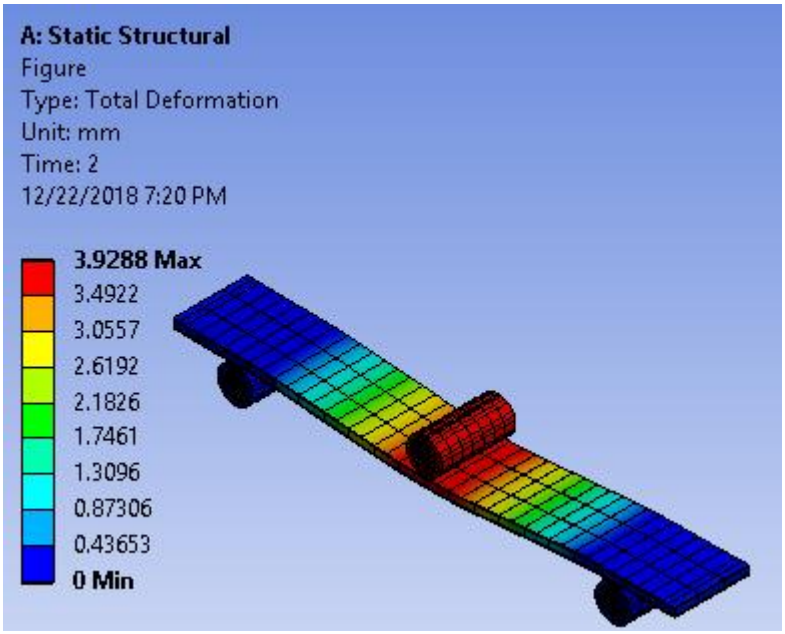

b) Thickness of 3mm sandwich sheet

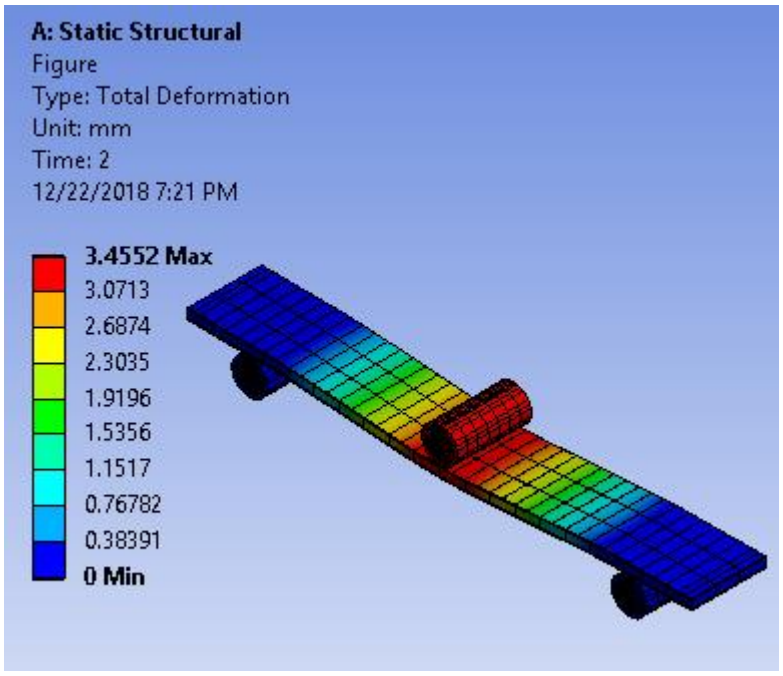

c) Thickness of 3.5mm sandwich sheet

Figure 5. 8 : Total Deformations for three thickness of sandwich laminates.

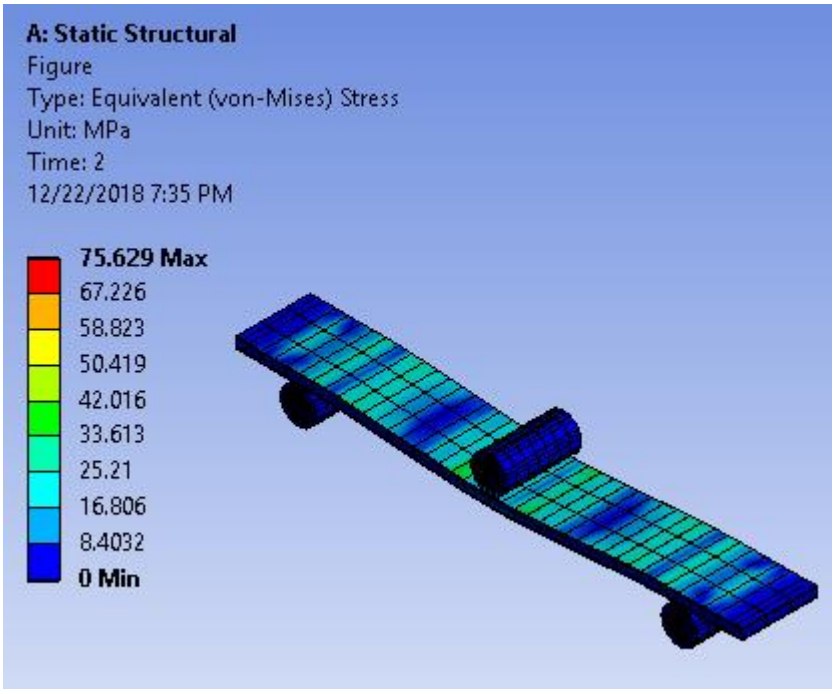

a) Thickness of 2.5mm sandwich sheet

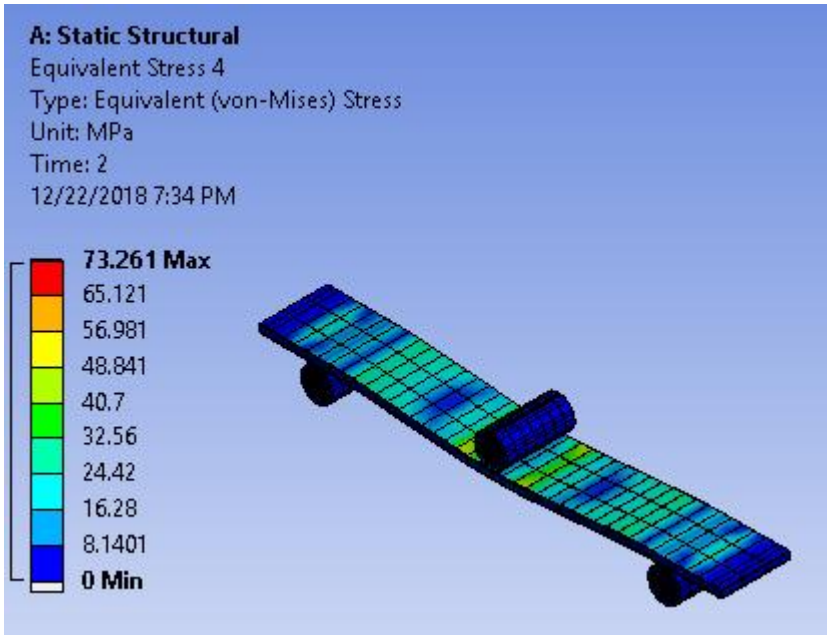

b) Thickness of 3mm sandwich sheet

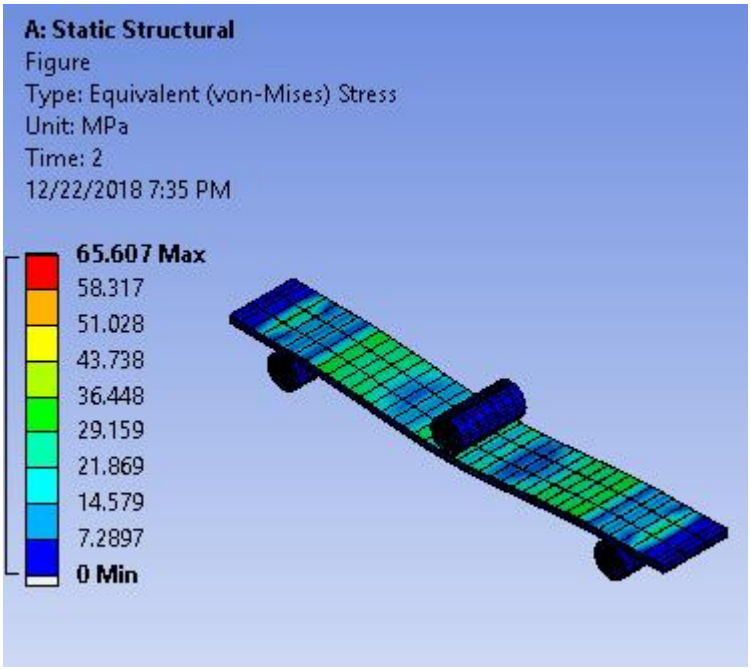

c) Thickness of 3.5mm sandwich sheet

Figure 5. 9 : Von Misses stress for three thickness of sandwich laminates.

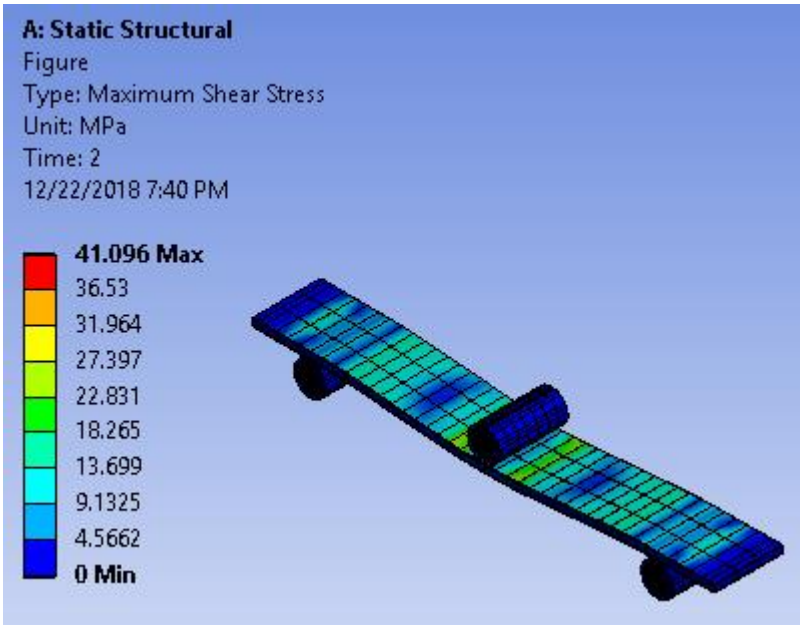

a) Thickness of 2.5mm sandwich sheet

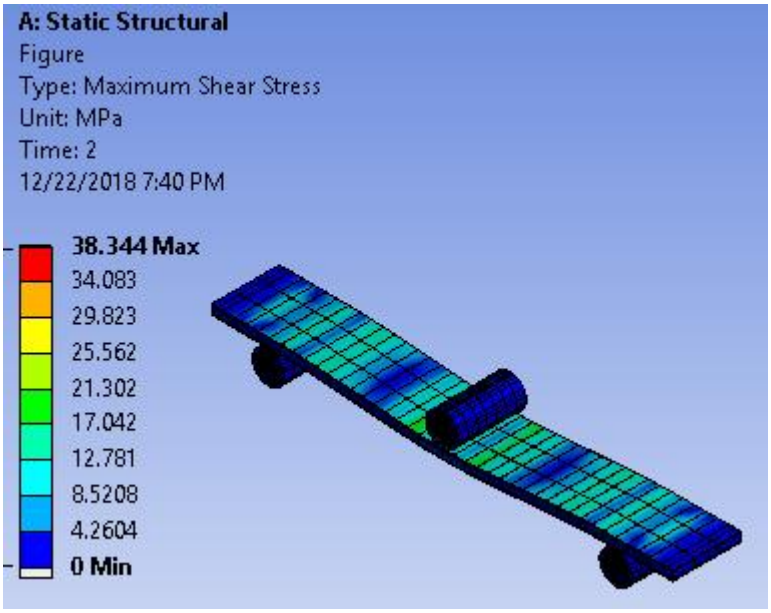

b) Thickness of 3mm sandwich sheet

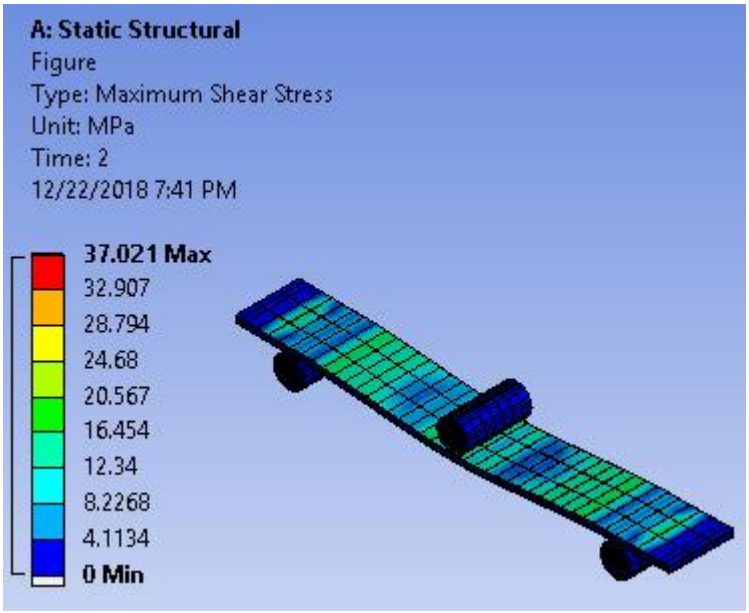

c) Thickness of 3.5mm sandwich sheet

Figure 5. 10 : Sher stress for different thickness of sandwich laminates

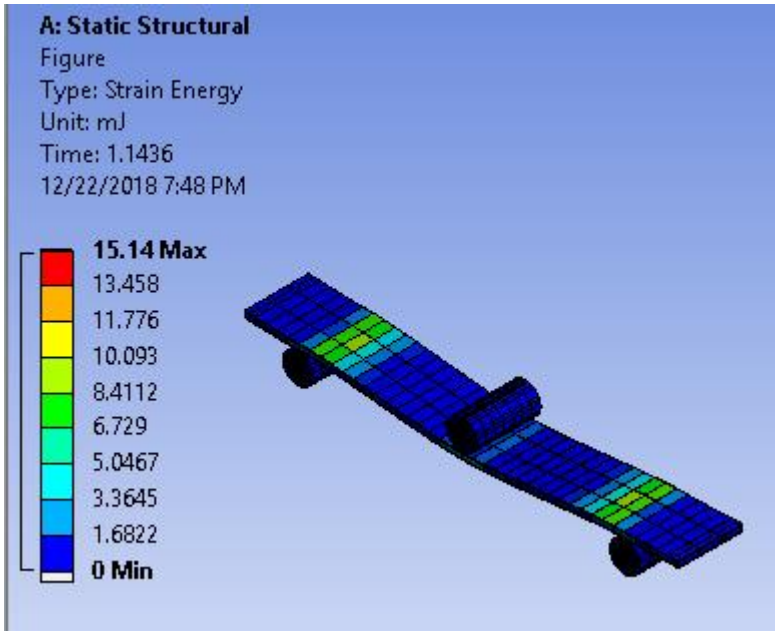

a) Thickness of 2.5mm sandwich sheet

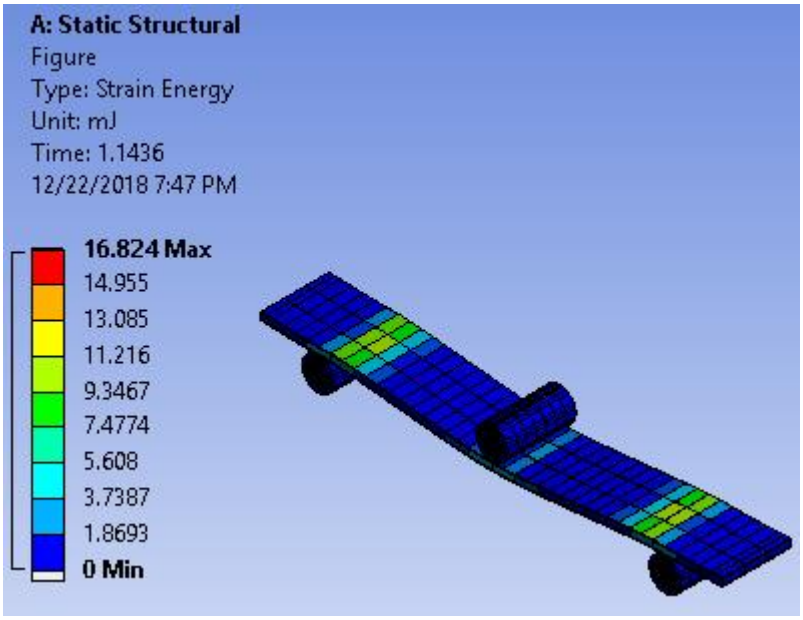

b) Thickness of 3mm sandwich sheet

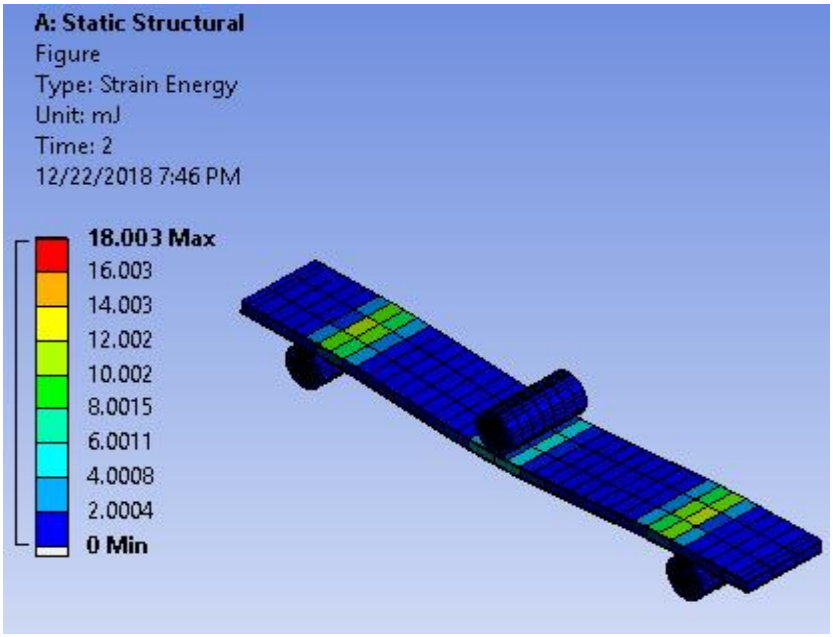

c) Thickness of 3.5mm sandwich sheet

Figure 5. 11 : Strain energy for different thickness of sandwich laminates

Deflection Vs thickness of sandwich sheets, stress Vs thickness of sandwich sheets and strain energy Vs time three different thickness of AA6061/HDPE/AA6061 sandwich sheets are analysis on figures 5.12,5.13 &5.14 within results taken from ANSYS simulation shown on appendix table A2.

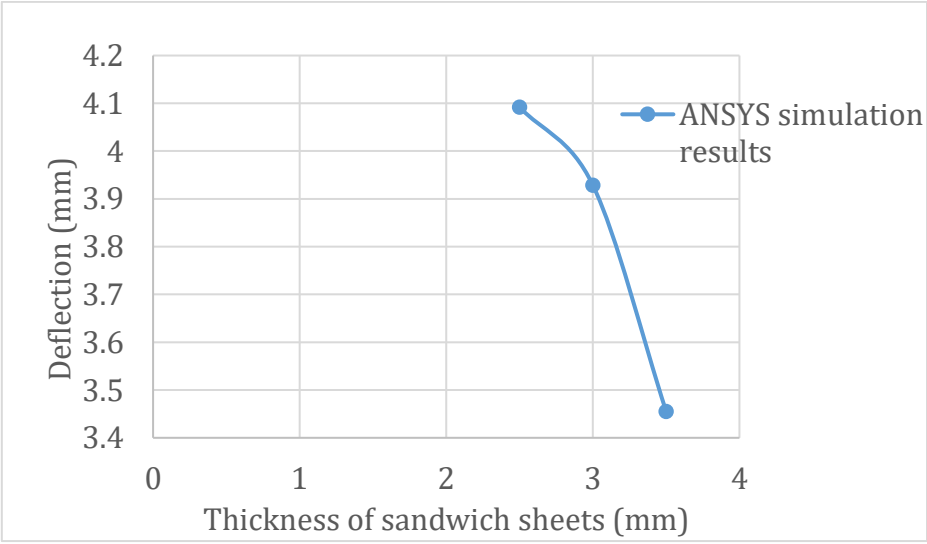

Figure 5. 12: Maximum deflection Vs thickness sandwich sheets.

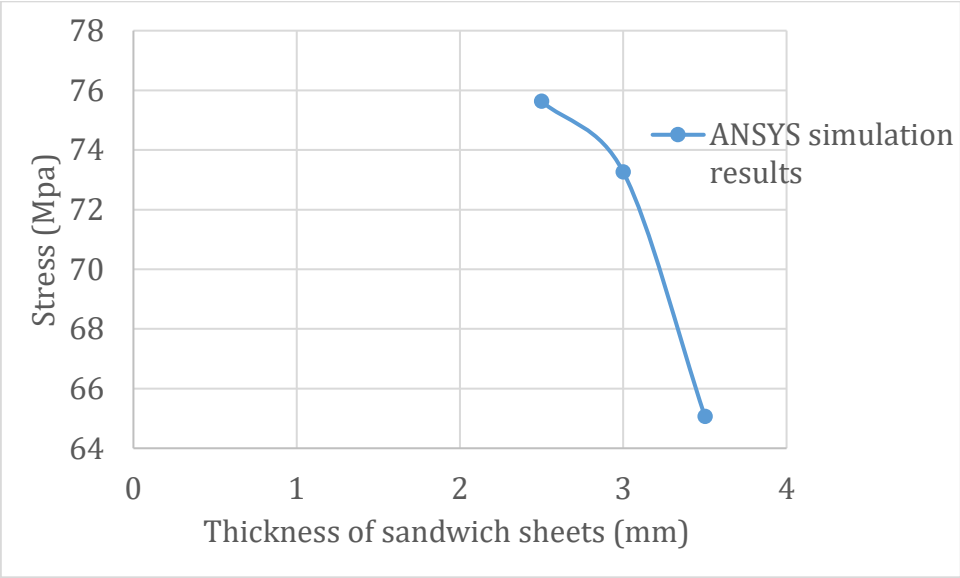

Figure 5. 13 : Equivalent von misses the stress Vs thickness of sandwich sheets.

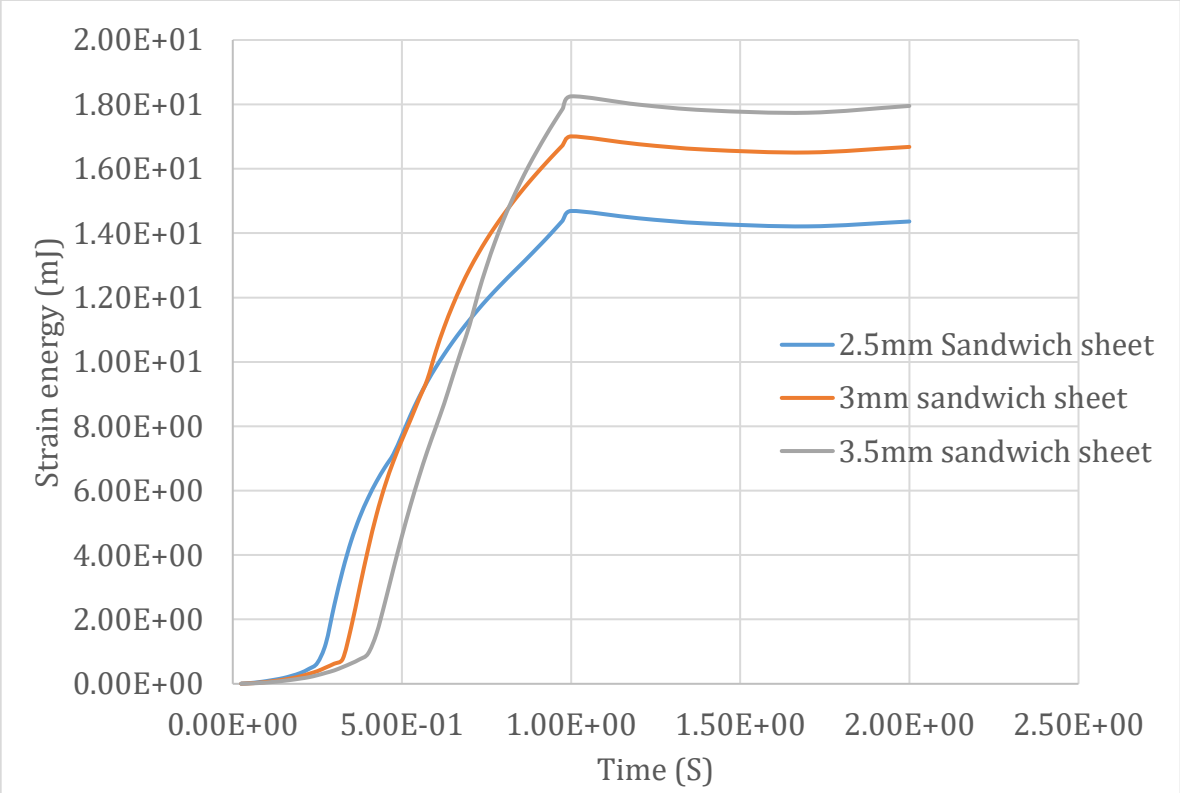

Figure 5. 14 : Three-point bending strain energy Vs time curve diagram

Figure 5.15 & 5.16 indicated that flexural stress and deflection of the sandwich sheets decrease with increasing the thickness of core sandwich materials. The results show that there are reasonably good agreements between the theoretical analysis and ANSYS simulation. This reasons due to the energy absorption of sandwich sheets increasing with the thickness of core materials as shown from the figure 5.14.

Generally, we conclude the core thickness of sandwich laminates in order to design directly proportional with the light weight of the material, high strength to weight ratio, cost performance, and pressure resist during the force applied. Compared with a monolithic metallic sheet, metal-plastic sandwich sheets offer lower density, higher specific flexural stiffness, better fire and sound resistance and vibration damping resistance characteristics.

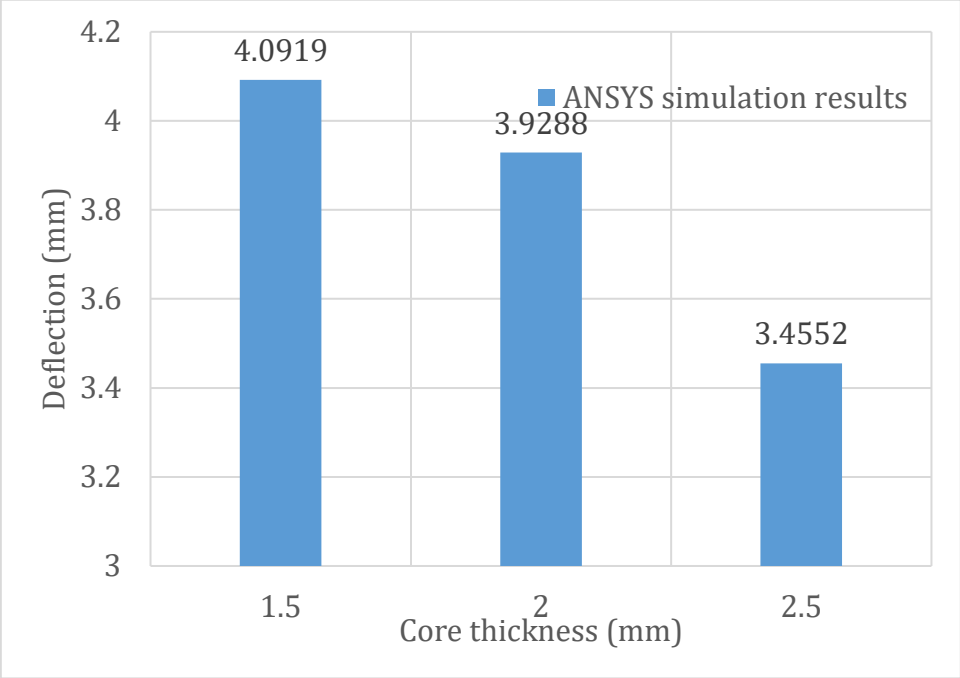

Figure 5. 15 : Maximum deflection value Vs core thickness of sandwich sheets

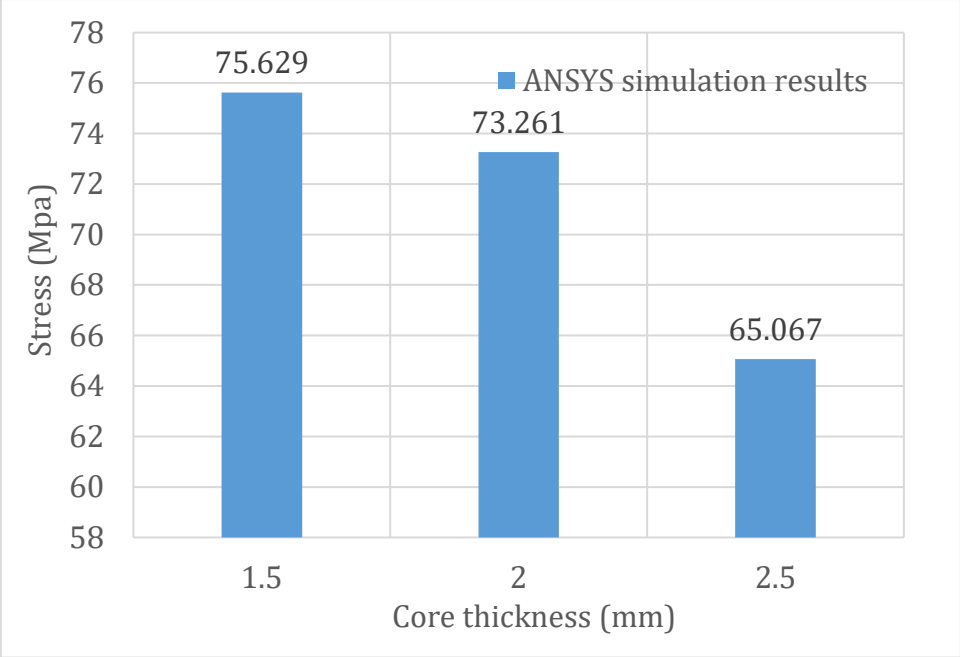

Figure 5. 16 : Maximum stress value Vs core thickness of sandwich sheets

5.1.5 Impact force simulation Results

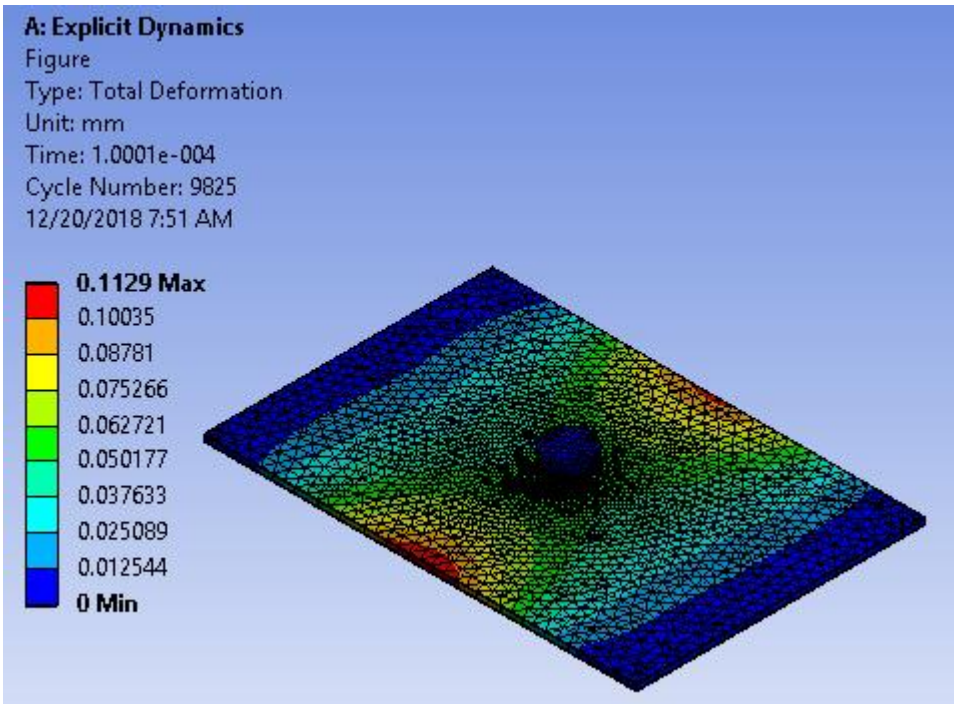

a) Thickness of 2.5mm sandwich sheet

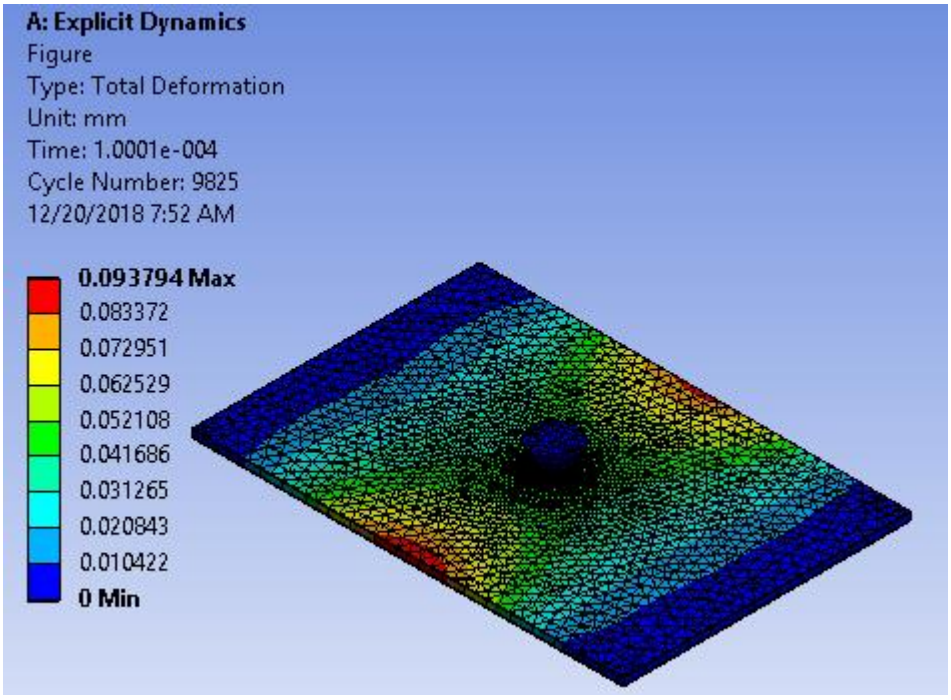

b) Thickness of 3mm sandwich sheet

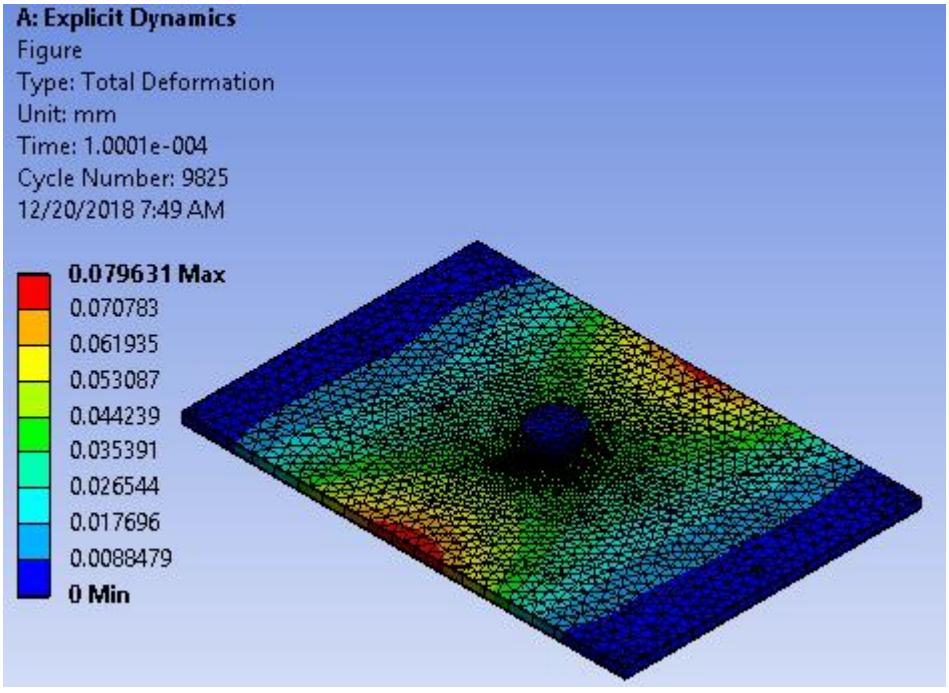

c) Thickness of 3.5mm sandwich sheet

Figure 5. 17 : Total deformations for different thickness of sandwich laminates.

Velocity Vs time three different thickness of AA6061/HDPE/AA6061 sandwich sheets are analysis on figure 5.18 within results taken from ANSYS simulation shown on appendix table A3

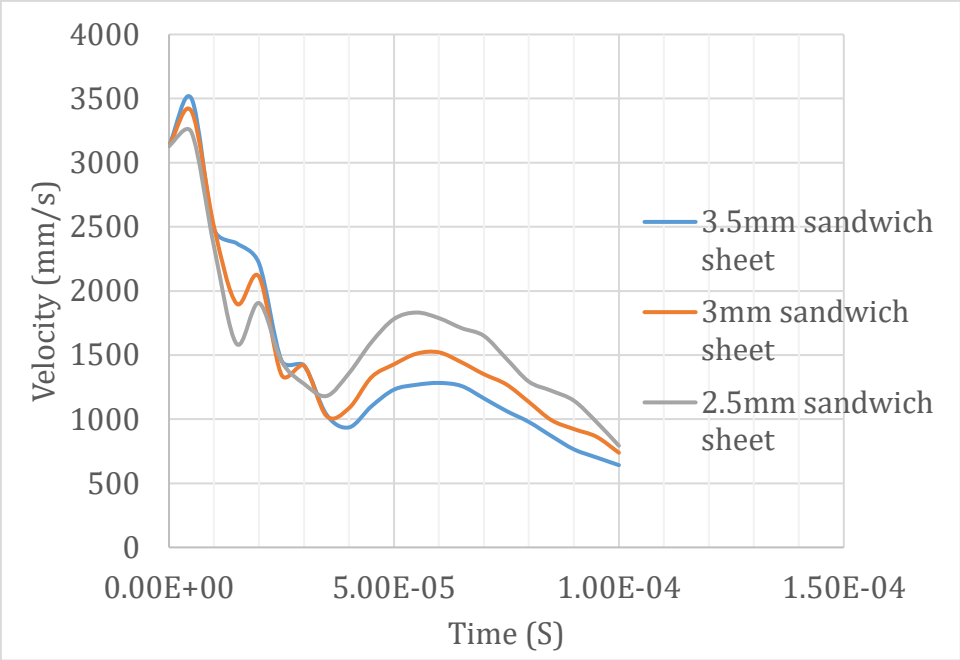

Figure 5. 18 : Velocity Vs time plots of the impact force simulation

The different velocities are plotted in Figure (5.18) in velocity-time graphs. It can be seen that the higher the starting velocity is, the faster the velocity decreases, which can be explained by the lack of damage criteria in the skin. Since the skin cannot be damaged, the indenter bounces back instead of perforating. Those theories can be justified from the above figure 5.17 the total deformation of sandwich sheets can be directly proportional to impact force. Because the internal energy of sandwich sheets depends on the thickness of core materials which stands for energy absorb. Those principle theories can be concluded according to the equation (4.6). Logically, higher impact energy result in higher deformation, both elastic and plastic deformation.

5.1.6 Cohesive zone model simulation result

A cohesive element based on damage mechanics, provided by ANSYS workbench, was used to model the delamination in laminates directly in terms of a traction-separation law. The available model in FEM assumes initially linear elastic response till interfacial strength, followed by damage initiation and evolution. Two major delamination modes exist the shear load delamination and the tensile load delamination. During deformation, one delamination mode or both of them may become active and may result in delamination of the layers.

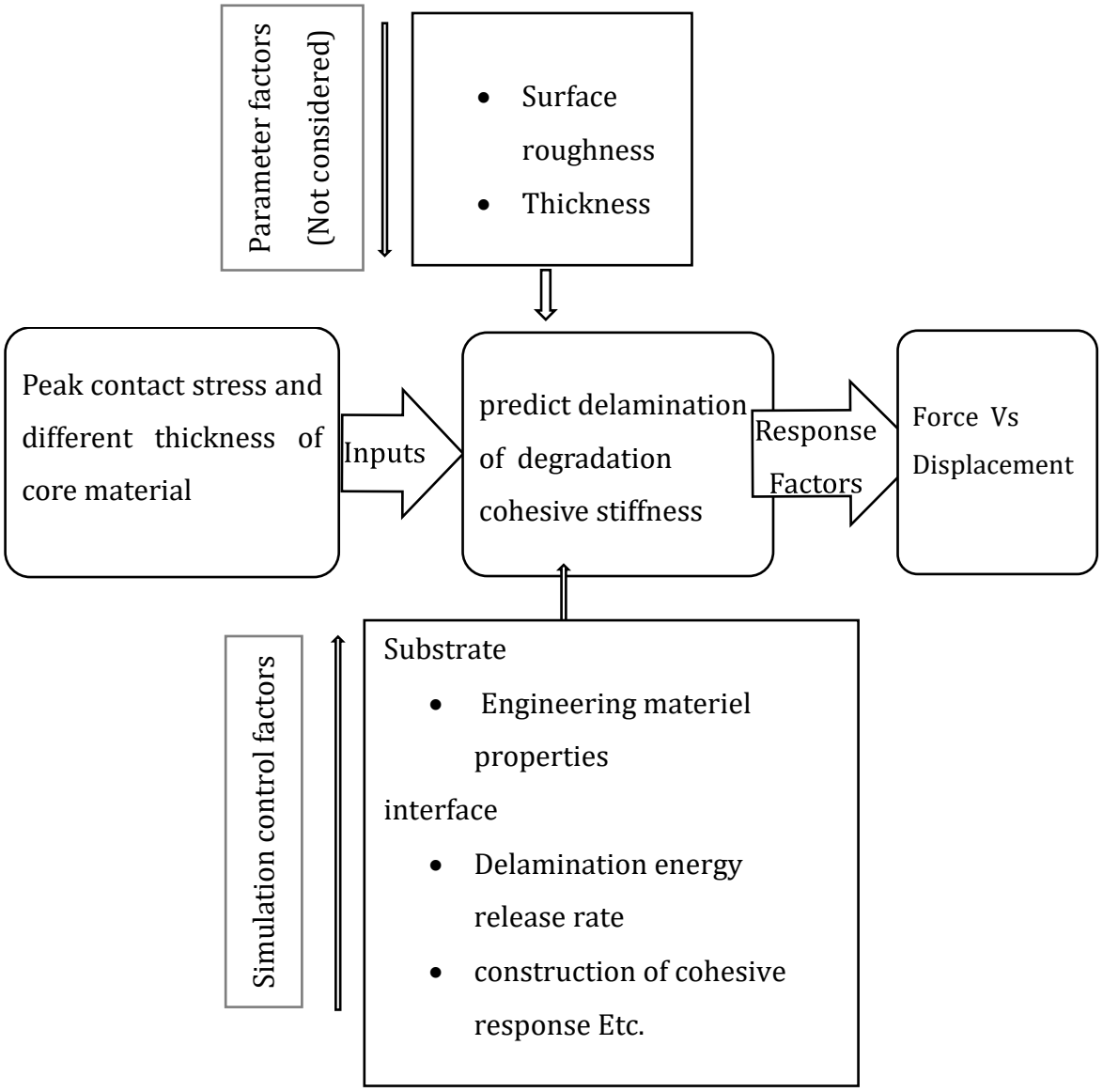

Figure 5. 19 : Delamination of sandwich sheets a traction-separation law parameter.

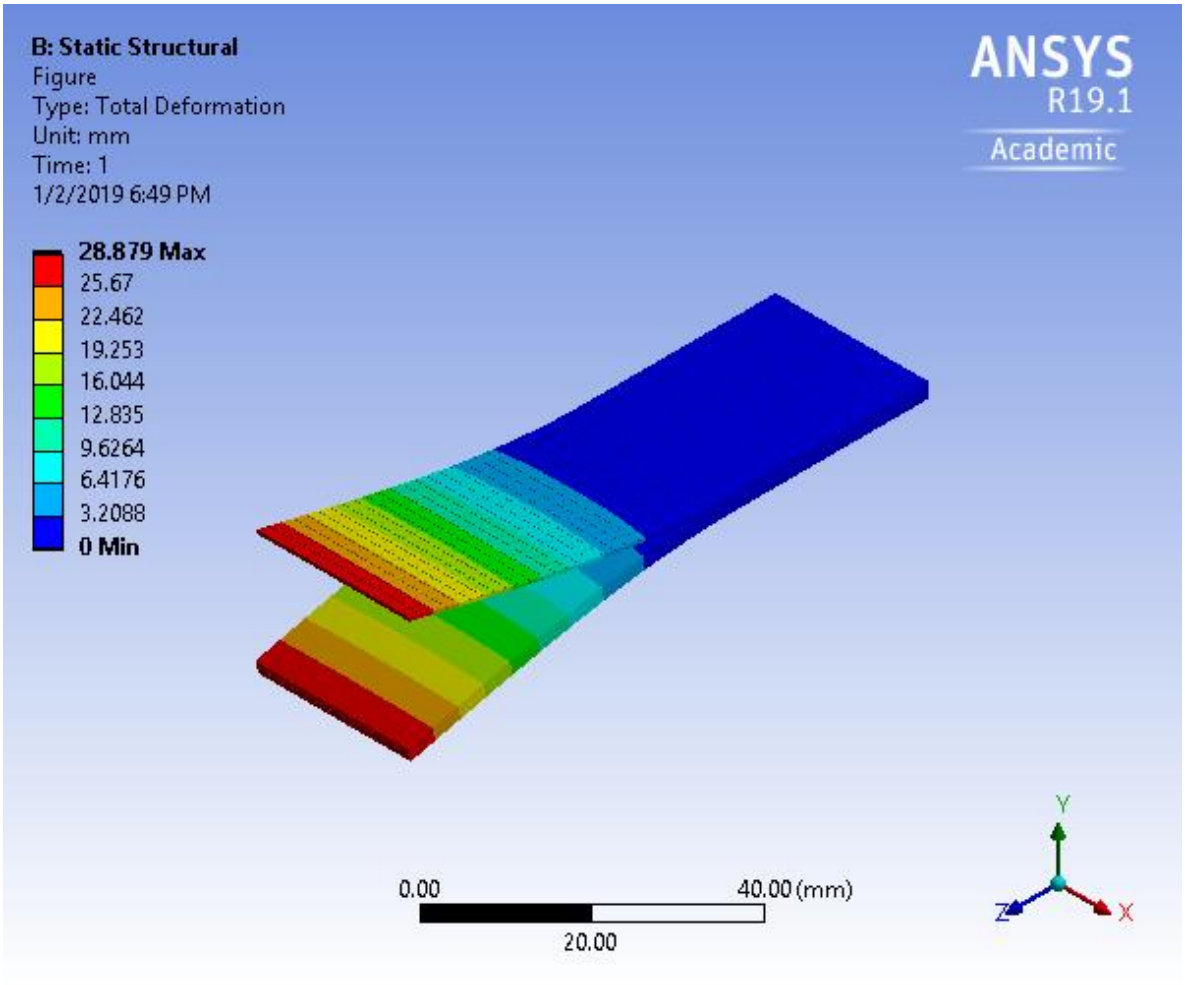

Figure 5. 20: Displacement simulation results

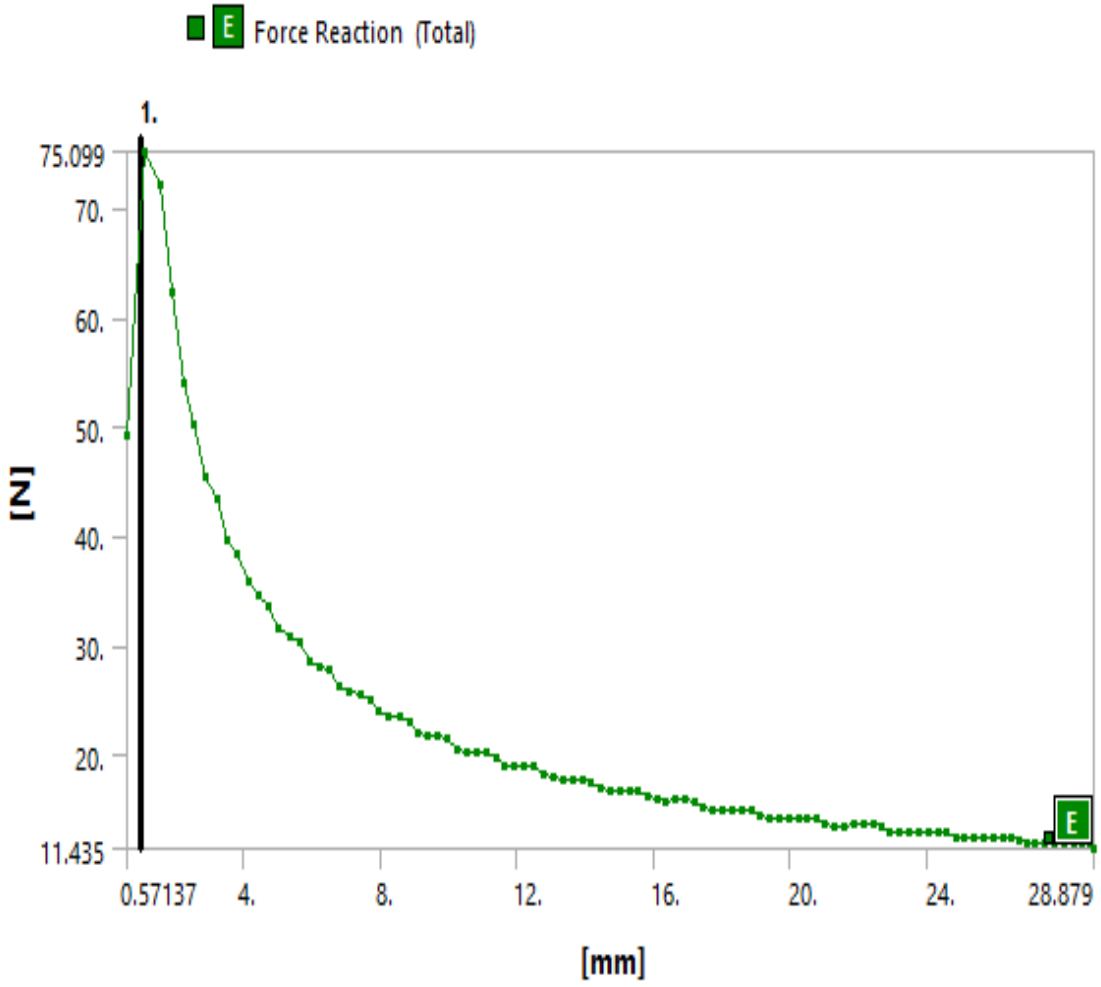

Figure 5. 21: Force Vs displacement graph curve simulation analysis.

The adhesion between the core and the metal sheets was investigated by T (90°) peel ANSYS simulation analysis. A typical force the average load Vs displacement responses the cohesive strength of between AA6061 and HDPE. The average peel strength can be calculated as;

$$\text{Average peel strength} = \frac{\text{Average load (N/mm)}}{\text{Bond width (mm)}} = \frac{75.099}{0.57137*25} = 5.25\text{Mpa} \quad (5.5)$$

Shown from figure 5.21 the area under the load Vs displacement cohesive zone model linear elastic traction separation law the damage initiation at the maximum point of force due to degradation of the cohesive stiffness. The maximum strength is 5.25Mpa at

point one which is derived from quadratic equation. The strength-based fracture model and the cohesive surface model are able to demonstrate the initial increase in force until reach the damage initiation. After the damage initiation, the force is inversely proportional to displacement due degradation of the cohesive stiffness.

The reason of damage initiation is

- Due to degradation of cohesive stiffness
- Imperfection bonding and
- Stress concertation

5.2 Comparison with the previous works

5.2.1 Tensile strength

The previous researcher's work indicates the elongation of tensile stress directly proportional to the thickness of core sandwich sheets [1] .which the results show that there are reasonably good agreements between the theoretical analysis and experimental work, which indicates that the rule of the mixture values. This principle predicts the elongation of AA6061/HDPE/AA6061 sandwich sheets increase with the increasing thickness of HDPE core sandwich sheets. This reasons can be defined as the core thickness of sandwich sheets stands for energy absorbs. To justify the tensile stress of the current work by experimental test and ANSYS Workbench simulation compared with the previous researcher's work shown from table 5.2.

Table 5. 2: Comparison with previous works on tensile properties of sandwich sheets

Skin	Core	Thickness of sandwich		Method	Tensile strength (Mpa)		Reference
					Experimental	ANSYS simulation	
AA6061	HDPE	2.5mm		ASTM D3039	50.3	57.3	**Current Work**
		3			49.5	52.02	
		3.5			47.4	48.8	
AA5052	HDPE	1.5		ASTM E8	74.7		[1]
		2			57.5		
		3			42.5		
		Rolling direction	Thickness (mm)				
AA8011 & AA1100	PP	0	2.82	ASTM E8/E8M	54.29		[49]
AA8011 & AA1100	PP	45	2.82	ASTM E8/E8M	39.8		
AA8011 & AA1100	PP	90	2.82	ASTM E8/E8M	45.56		
AA8011 & AA1100	PP	Average	2.82	ASTM E8/E8M	46.55		

5.2.2 Flexural Strength

The previous researcher's work indicates flexural strength directly proportional to the thickness of core sandwich sheets [50]. which the results show that there are reasonably good agreements between the theoretical analysis and Experimental work, which indicates that the rule of the mixture can appropriately predict the flexural stress and deflection inversely proportional with the thickness of core sandwich sheets. This reasons can be defined as the core thickness of sandwich sheets stands for energy absorbs. To justify the flexural properties of the current work by ANSYS Workbench simulation compared with the previous researcher's work shown from table 5.3. which flexural stress and deflection of the sandwich sheets inversely proportional with the thickness of core sandwich materials.

Table 5. 3 : Comparison with previous works on Flexural properties of Sandwich sheets

Skin	Core	Thickness (mm)	Load P (N)	Method	Bending strength (Mpa)	Reference
AA6061	HDPE	2.5	250	ANSYS software	75.629	Current Work
		3	250	ANSYS software	73.26	
		3.5	250	ANSYS software	65.07	
AA8011& AA1100	pp	2.82	140	ASTM D790	81.56	[49]

Chapter 6

Conclusions and recommendation

6.1 Conclusions

The mechanical properties of AA6061/HDPE/AA6061 sandwich sheets agree with the experimental test, ANSYS simulation and rule of the mixture following conclusions are obtained.

- The density test specimen of sandwich sheets decreases with increasing the thickness of the HDPE layer. This principle can be justified both experimental weight balance and mathematical modeling rule of mixture.
- The hardness of AA6061/HDPE/AA6061 sandwich sheet is higher than that of the monolithic AA6061 sheet and it increases with increasing the thickness of HDPE core.
- The elongation of AA6061/HDPE/AA6061 sandwich sheets increasing with increasing the thickness of HDPE core.
- Flexural stress and deflection of the sandwich sheets decrease with increasing the thickness of HDPE core.
- The impact force resistance increase with increasing the thickness of HDPE core.
- Analysis of crash structures consisting of MPM sandwich structures with a thermoplastic core exhibit a sufficient energy absorbing effectiveness, comparable or even better than metallic crash absorbers.
- The area under the load Vs displacement cohesive zone model linear elastic traction separation law the damage initiation at the maximum point of force due to degradation of the cohesive stiffness.
- The strain energy absorption of sandwich sheets increasing with the thickness of core materials which resist impact force.
- Generally, we conclude the core thickness of sandwich laminates in order to design directly proportional with the light weight of the material, high strength to weight ratio, cost performance, and pressure resist during the force applied.

6.2 Recommendation

The following study of sandwich sheets application to finding the possibility of the appropriate the core thickness of sandwich laminates in order to design directly proportional with the light weight of the material, high strength to weight ratio, cost performance and pressure resist during the force applied. The following studies could be performed to analyse more details on this topic.

- Analyse of the formability of sandwich sheets for different application
- Dynamic and statically load Analysis Metal/Polymer/metal Sandwich Composites
- Rivet joint Analysis Metal/Polymer/metal Sandwich Composites
- Study on fracture properties of the composite material
- Study on optimization of mechanical properties
- Study on fire resistance properties
- Study experimental three point, impact force and traction separation with simulation.

References

[1] J. Liu and W. Xue, "Formability of AA5052 / polyethylene / AA5052 sandwich sheets," *Trans. Nonferrous Met. Soc.*, vol. 23, pp. 964–969, 2013.

[2] S. Mousa, "Roll bonding of metal-polymer-metal sandwich composites," *Grad. Theses Diss.*, pp. 1–50, 2017.

[3] S. A. Makhmale, S. B. Patil, and V. G. Kale, "Automobile Bodies By Advance Material With Light Weight," *Eng. Technol.*, vol. 03 Issue, pp. 970–975, 2016.

[4] D. G. Vamja and G. G. Tejani, "Experimental Test on Sandwich Panel Composite Material," *ijirset.com*, vol. 2, no. 7, pp. 3047–3054, 2013.

[5] J. Liu, W. Liu, and W. Xue, "Forming limit diagram prediction of AA5052 / polyethylene / AA5052 sandwich sheets," *Mater. Des.*, vol. 46, pp. 112–120, 2013.

[6] H. P. Prof, "Three-layered sandwich material for lightweight applications," *Emerg. Mater. Res.*, vol. 3, pp. 130–135, 2014.

[7] S. A. Nikolaevich, A. A. Valerievich, G. A. Igorevich, S. A. Alexandrovich, and S. M. Alexandrovich, "Advanced materials of automobile bodies in volume production," *Eur. Transp. /*, vol. 10, no. 56, pp. 1–27, 2014.

[8] E. Ghassemieh, "Materials in Automotive Application , State of the Art and Prospects," *New Trends Dev. Automot. Ind.*, vol. 8, pp. 366–394, 2011.

[9] S. M. Ahmed, "A Review on Fibre Metal Laminate Sandwitch Panel," *Eng. Trends Technol.*, vol. 40, no. 1, pp. 11–14, 2016.

[10] S. C. Materials and F. C. Campbell, "Introduction to Composite Materials," *Struct. Compos. Mater.*, pp. 1–28, 2010.

[11] D. Lukkassen and A. Meidell, "Advanced Materials and Structures and their Fabrication Processes," 2007.

[12] J. S. and M. NardinC, "Theories and Mechanisms of Adhesion," *Physico-Chimie des Surfaces Solides*, pp. 1–999, 2003.

[13] F. Ferrari and F. Ferrari, "Lightweight Metal / Polymer / Metal Sandwich Composites for Automotive Applications," *Electron. Theses Diss.*, no. 7256, pp. 1–126, 2017.

[14] Ganesh, "Tensile and compressive testing," *Compos. Mater.*, vol. 8, no. 18, pp. 1–

16, 2014.

[15] B. A. Brent and S. Brigham, “History of Composite Materials — Opportunities and Necessities,” *Historical Perspectives of Composites,*. pp. 1–8, 1990.

[16] E. Mangino, J. Carruthers, and G. Pitarresi, “The Future Use of Structural Composite Materials in the Automotive Industry,” *Int. J. Veh. Des.*, vol. 44, no. 3/4, p. 211, 2007.

[17] A. C. Panels, R. Tinto, and A. C. P. There, “Aluminium Composite Panels,” *History of ACP*. pp. 1–7, 2000.

[18] S. N. A. A. M. H. Parsa, M. Ettehad, “FLD Determination of AA3105 / PP / AA3105 Sandwich Sheet Using Numerical Calculation and Experimental Investigation,” *Int. J. Mater. Form.*, no. May 2014, pp. 1–9, 2009.

[19] M. Harhash and Heinz Palkowski, “Mechanical Properties and Forming Behaviour of Laminated Steel / Polymer Sandwich Systems with local inlays – Part 1,” *Compos. Struct.*, vol. 118, no. August, pp. 112–120, 2014.

[20] H. P. Mohamed Harhash, “Deep-And Stretch-Forming of Steel / Polymer / Steel Laminates,” in *Composite Materials*, 2016, no. April, pp. 69–74.

[21] D. Hara and G. O. Özgen, “Investigation of Weight Reduction of Automotive Body Structures with the Use of Sandwich Materials,” *Transp. Res. Procedia*, vol. 14, pp. 1013–1020, 2016.

[22] J. Liu and W. Xue, “Unconstrained Bending and Springback Behaviors of Aluminum-Polymer Sandwich Sheets,” *Adv. Manuf. Technol.*, vol. 91, no. 5–8, pp. 1517–1529, 2017.

[23] A. Kami, B. M. Dariani, D. S. Comsa, and D. Banabic, “an Experimental Study on the Formability of a Vibration Damping Sandwich Sheet (Bondal),” vol. 18, no. 3, pp. 281–290, 2017.

[24] A. C. and H. P. V. Harms, M. Harhash, “Energy Absorption Behavior of Metal / Polymer / Metal Sandwich Crash Structures,” *Key Eng. Mater.*, vol. 746, no. ISSN: 1662-9795, pp. 275–281, 2017.

[25] C. Jang *et al.*, “Material property of metal skin of – sheet molding compound structures for the production lightweight vehicles body laminate frame,” *Procedia Eng.*, vol. 207, pp. 878–883, 2017.

[26] : Luca Quagliato, “Steel skin – SMC laminate structures for lightweight automotive manufacturing,” *J. Phys. Conf. Ser*, vol. 896, pp. 1–8, 2017.

[27] J. Wilson and C. Maritime, “Light Alloys,” *Spring Sci.*, pp. 1–10, 1998.

[28] U. Tamilarasan and L. Karunamoorthy, “Mechanical Properties Evaluation of the Carbon Fibre Reinforced Aluminium Sandwich Composites,” *Mater. Res.*, vol. 18, no. 5, pp. 1029–1037, 2015.

[29] E. P. M. T. FORCE, “Packing Materials Polyethylene for Food Packing Applications,” in *International Life Sciences*, 2003.

[30] W. R. R. Kawawada, Karen, “Polyethylene,” *Wikipedia*. (22 May 2008, pp. 1–84, 2008.

[31] E. Newport, Isle of Wight, “SP Systems Guide to Composites,” *SP Syst. Mater. Compos. Eng.*, pp. 1–64.

[32] M. A. Ghafaar, “Application of the Rule of Mixtures and Halpin-Tsai Equations to Woven Fabric Reinforced Epoxy Composites,” *Eng. Sci.*, vol. 34, no. 1, pp. 227–236, 2005.

[33] H. Palkowski, O. A. Sokolova, and A. Carrad, “Sandwich Materials,” *Automotive Engineering*. pp. 1–14, 2004.

[34] M. Pipe and S. Pty, “HDPE Physical Properties,” *Marley pipe systems*, vol. 2. pp. 1–10, 2010.

[35] C. Balama and L. Mbwambo, “Strength Properties of Chipboards Available Tanzania Market,” *For. Nat. Conserv.*, vol. 82, no. 1, pp. 1–10, 2012.

[36] de S. Paulo, “Standard Hardness Conversion Tables for Metals Relationship Among Brinell Hardness , Vickers Hardness , Rockwell Hardness , Superficial Hardness , Knoop Hardness , Scleroscope Hardness , and Leeb Hardness 1,” no. 21, pp. 1–21, 2017.

[37] E. E.LEVI, “Practical Hardness Testing,” *Am. Soc. Test. Mater.*, pp. 1–22, 2003.

[38] R. Rametta, A. Passaro, L. Lanzilotto, and A. Maffezzoli, “Effect of the Manufacturing Process and Skin-Core Adhesion Efficiency on the Mechanical Properties of a Thermoplastic Sandwich,” *Eng. Innov.*, vol. 2, no. 6, pp. 1–10, 2014.

[39] J. Arbaoui, Y. Schmitt, J. Pierrot, and F. Royer, “Comparison Study and Mechanical Characterisation of a Several Composite Sandwich Structures,”

sapub.org/cmaterials, vol. 5, no. 1, pp. 1–8, 2015.

[40] D. L. Hunston, "Assessment of Sandwich Beam in Three-Point Bending for Measuring Adhesive Shear," *Natl. Inst. Stand. Technol.*, vol. 123, no. July, pp. 322–328, 2001.

[41] K. Logesh, "Review on manufacturing of fibre metal laminates and its characterization techniques," *IJMET*, vol. 8, no. 10, pp. 561–578, 2017.

[42] R. Kulkarni and A. Mache, "A Review : Fiber Metal Laminates (FML ' s) - Manufacturing , Test methods and Numerical modeling," *Eng. Technol. Sci.*, vol. 6, no. 1, pp. 71–84, 2016.

[43] N. A. Apetre, B. V Sankar, and D. R. Ambur, "Low-velocity Impact Response of Sandwich Beams with Functionally graded core," *Solids Struct.*, vol. 43, no. 20, pp. 2479–2496, 2006.

[44] J. Wang, Q. H. Qin, Y. L. Kang, X. Q. Li, and Q. Q. Rong, "Mechanics of Materials Viscoelastic adhesive interfacial model and experimental characterization for interfacial parameters," *Mech. Mater.*, vol. 42, no. 5, pp. 537–547, 2010.

[45] P. Fuchs, S. Stelzer, K. Fellner, H. Pothukuchi, and G. Pinter, "Simulation of Delamination in Composites," *Polyregion Leoben*, vol. 24, no. March, 2015.

[46] M. Khoshravan, "Cohesive Zone Parameters Selection for Mode-I Prediction of Interfacial Delamination," *Orig. Sci. Pap. Receiv.*, vol. 61, pp. 507–516, 2015.

[47] G. Giuliese, A. Pirondi, and F. Moroni, "A cohesive zone model for three-dimensional fatigue debonding / delamination," *Procedia Mater. Sci.*, vol. 3, pp. 1473–1478, 2014.

[48] M. Alfano, F. Furgiuele, G. Lubineau, and G. H. Paulino, "Simulation of debonding in Al / epoxy T-peel joints using a potential-based cohesive zone model," *Procedia Eng.*, vol. 10, pp. 1760–1765, 2011.

[49] C. Techniques, K. Logesh, T. Nadu, and T. Nadu, "Investigation of Mechanical Properties of AA8011 / PP / AA1100 Sandwich Materials," *ChemTech Res.*, vol. 6, no. 3, pp. 1749–1752, 2014.

[50] B. V. Ramnath, C. Elanchezhian, J. M. P. Martins, P. M. Cunha, Y. M. Hwang, and C. Y. Chang, "Finite Element Analysis of Mild Steel - Rubber Sandwich Composite Material," *IOP Conf.Materials Sci. Eng.*, vol. 3, pp. 1–10, 2018.

Appendix

Experimental and FEM simulation tensile Results

Mechanical properties of sandwich sheets were determined through conducting the tensile tests. The engineering strain-nominal stress curves of sandwich sheets determined by with breaking points.

The experimental tensile test was done in Ethiopian Conformity Assessment Enterprise shown as below with certificate results.

Ductile failure of sandwich sheets.

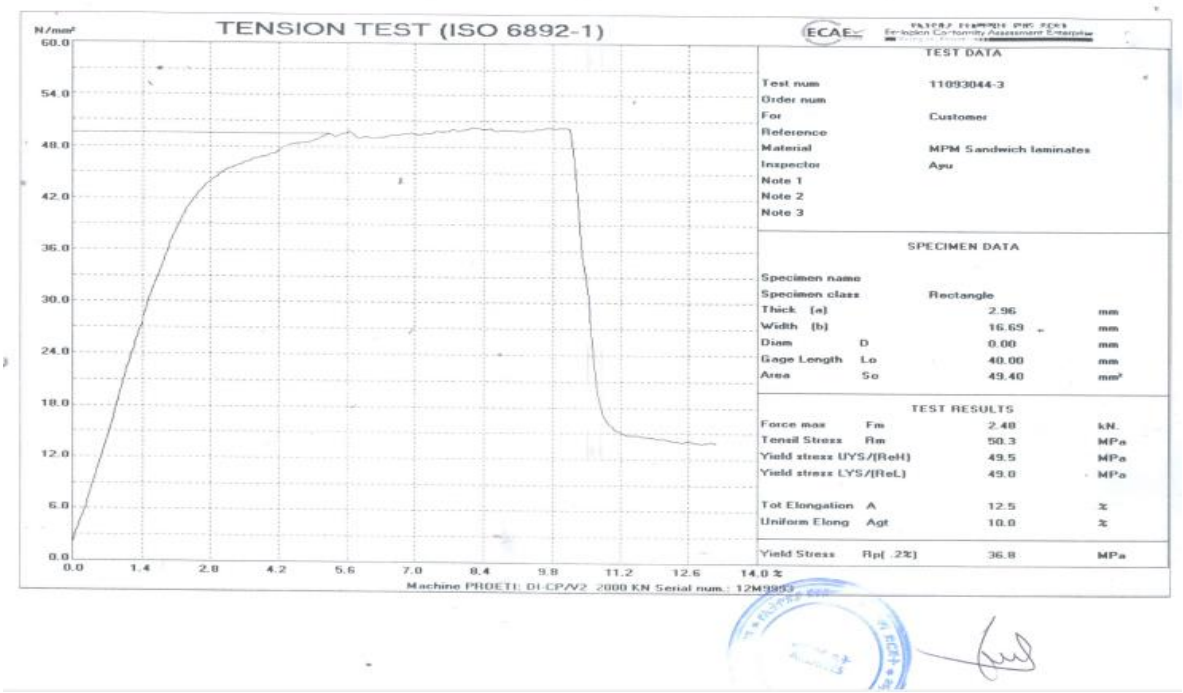

stress Vs strain engineering curves for 2.5mm sandwich sheet

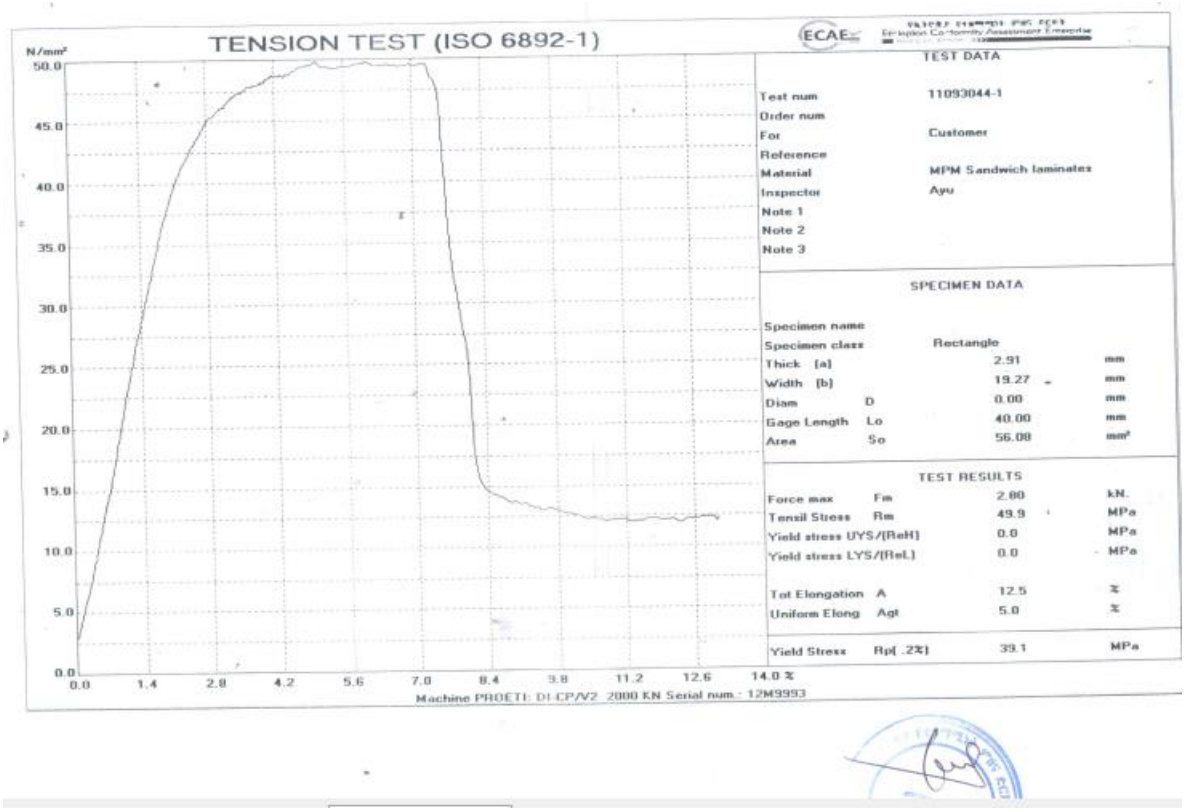

Stress Vs strain engineering curves for 3mm sandwich sheet

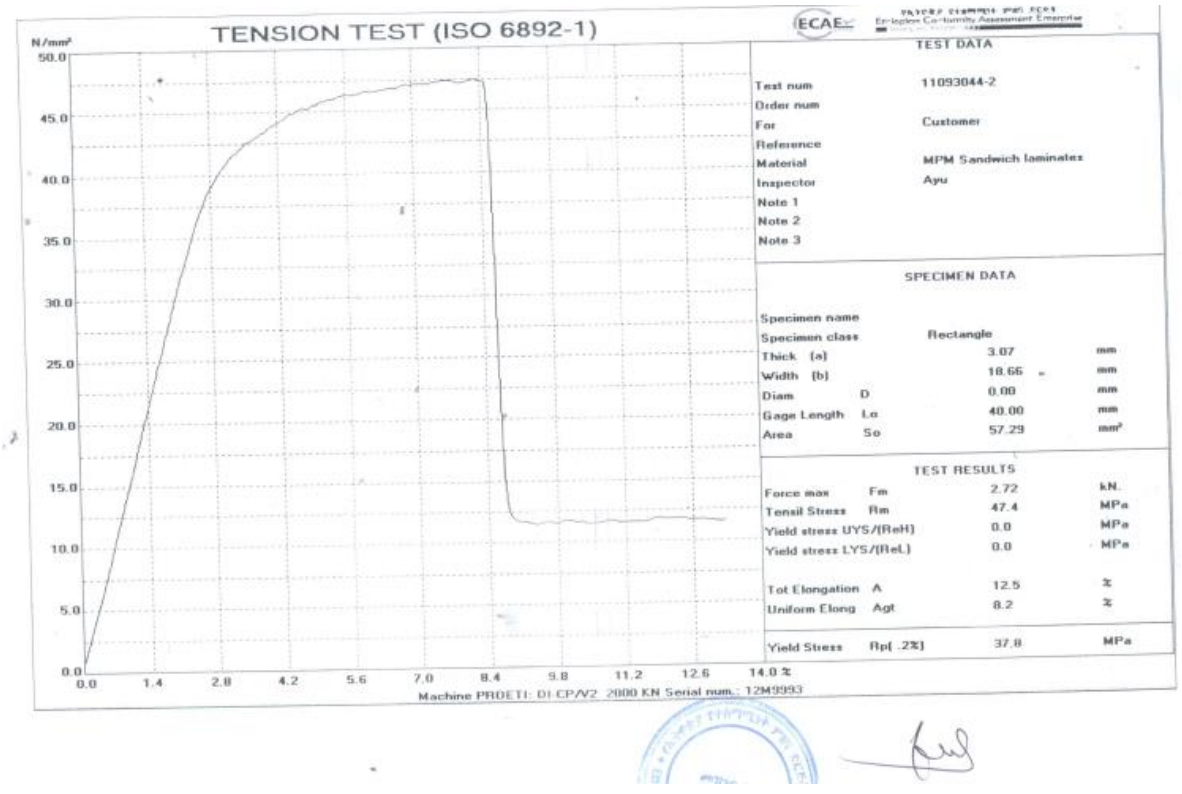

Stress Vs strain engineering curves for 3.5mm sandwich sheet

Table A1: Iteration data collected tensile strength during experimental tests and ANSYS simulations

Experimental test results Thickness of sandwich sheets						ANSYS Workbench simulation results Thickness of sandwich sheets					
2.5mm		3mmm		3.5mm		2.5mm		3mm		3.5mm	
Strain (%)	Stress (Mpa)	Strain (%)	Stress (Mpa)	Strain (%)	Stress (Mpa)	Strain (%)	Stress (Mpa)	Strain (%)	Stress (Mpa)	Strain (%)	Stress (Mpa)
0.00E+00	5.5862	0.00E+00	5	0.00E+00	4.8	0.00E+00	5.2	0.00E+00	5	0.00E+00	4.8
2.00E-01	11.172	2.00E-01	11	2.00E-01	10.5	2.00E-01	10	2.00E-01	11	2.00E-01	10.5
4.00E-01	16.759	4.00E-01	14	4.00E-01	13	4.00E-01	14.5	4.00E-01	14	4.00E-01	13
1.20E+00	39.104	1.20E+00	35	1.20E+00	34	1.20E+00	37	1.20E+00	35	1.20E+00	34
1.50E+00	44	1.50E+00	40	1.50E+00	39	1.50E+00	41	1.50E+00	39	1.50E+00	38
1.70E+00	47	1.70E+00	42	1.70E+00	41	1.70E+00	45	1.70E+00	41	1.70E+00	40
2.30E+00	51	2.30E+00	46	2.30E+00	44	2.30E+00	50	2.30E+00	45	2.30E+00	43
3.50E+00	53	3.50E+00	48.8	3.50E+00	46.5	3.50E+00	52	3.50E+00	47	3.50E+00	45

4.00E+00	53.5	4.00E+00	49.5	4.00E+00	47	4.00E+00	52.5	4.00E+00	47.5	4.00E+00	46
4.50E+00	54	4.50E+00	50	4.50E+00	47.5	4.50E+00	53	4.50E+00	48	4.50E+00	46.5
5.50E+00	56	5.50E+00	51.2	5.50E+00	47.8	5.50E+00	54	5.50E+00	49.5	5.50E+00	46.8
6.00E+00	56.4	6.00E+00	51.5	6.00E+00	48	6.00E+00	54.5	6.00E+00	50	6.00E+00	47
6.50E+00	56.6	6.50E+00	51.8	6.50E+00	48.5	6.50E+00	54.8	6.50E+00	50	6.50E+00	47.5
7.00E+00	57	7.00E+00	52	7.00E+00	49	7.00E+00	55	7.00E+00	50.5	7.00E+00	48
7.50E+00	56	7.50E+00	51.5	7.50E+00	48.3	7.50E+00	55	7.50E+00	50	7.50E+00	47.2
8.20E+00	54	8.20E+00	50.5	8.30E+00	45	8.20E+00	53	8.20E+00	47	8.30E+00	44
8.30E+00	46.931	8.40E+00	44.733	8.50E+00	42	8.30E+00	46.931	8.40E+00	40	8.50E+00	35
8.40E+00	23	8.70E+00	21	8.80E+00	18	8.40E+00	22	8.70E+00	20	8.80E+00	17
1.10E+01	22.479	1.25E+01	20.045	1.35E+01	17.5	1.10E+01	21	1.25E+01	19	1.35E+01	16
1.25E+01	22	1.35E+01	20	1.40E+01	17	1.25E+01	20.5	1.35E+01	19.5	1.40E+01	15.5

Table A2: Iteration data analysis three point bending during ANSYS simulations

Thickness of sandwich sheets									
	2.5mm			3mm			3.5mm		
Time (s)	Stress (Mpa)	Total deformation(mm)	Strain energy (mJ)	Total deformation(mm)	Stress (Mpa)	Strain energy (mJ)	Total deformation(mm)	Stress (Mpa)	Strain energy (mJ)
2.50E-02	12.606	0.12332	5.51E-03	0.11332	11.606	3.61E-03	0.11332	10.606	2.53E-03
0.1	54.143	0.25218	8.56E-02	0.23218	53.143	5.80E-02	0.23218	51.143	4.08E-02
0.375	51.801	0.93103	5.171	0.93103	51.801	2.9851	0.93103	51.801	0.76057
0.4	56.554	1.0685	5.772	1.0685	56.554	4.186	1.0685	56.554	0.94008
0.55	63.113	1.7797	8.8897	1.7797	63.113	8.8306	1.7797	63.113	6.4106
0.625	66	2.4573	10.237	2.4573	66	11.082	2.4573	64	8.7072
0.675	66.396	2.7839	10.973	2.7839	66.396	12.348	2.522	63.396	10.346
0.7	66.939	2.9207	11.304	2.9207	66.939	12.882	2.533	62.939	11.144
0.725	65.268	3.0451	11.623	3.0451	63.268	13.357	3.605	63.268	12.111
0.875	66.676	3.1587	13.269	3.1587	64.676	15.574	2.66	64.676	16.091
1.4	75	3.9395	14.3	3.9395	73.261	16.594	3.244	65	17.817
1.7	65.109	4.0461	14.21	3.88	64.109	16.506	3.332	65.607	17.741
2	59.923	4.0919	15.14	3.9288	58.923	16.824	3.4552	59.923	18.003

Table A3: Iteration data analysis impact force ANSYS simulations

Thickness of sandwich sheets					
2.5mm		3mm		3.5mm	
Time (S)	Velocity (mm/s)	Time (S)	Velocity (mm/s)	Time (S)	Velocity (mm/s)
1.18E-38	3131.5	1.18E-38	3131.5	1.18E-38	3131.5
5.00E-06	3235.9	5.00E-06	3400	5.00E-06	3499.3
1.00E-05	2344.1	1.00E-05	2497.6	1.00E-05	2480.8
2.50E-05	1451.7	2.50E-05	1345.3	2.50E-05	1457.7
3.00E-05	1275.8	3.00E-05	1416.7	3.00E-05	1418.7
4.50E-05	1600.1	4.50E-05	1327.2	4.50E-05	1100.7
5.00E-05	1781	5.00E-05	1427.7	5.00E-05	1230.3
6.50E-05	1710.2	6.50E-05	1443.7	6.50E-05	1258.8
7.00E-05	1649.5	7.00E-05	1350.5	7.00E-05	1162.1
7.50E-05	1471.3	7.50E-05	1270.6	7.50E-05	1063.8
8.00E-05	1292.4	8.00E-05	1133.5	8.00E-05	978.11
8.50E-05	1221.7	8.50E-05	992.63	8.50E-05	868.51
9.50E-05	978.71	9.50E-05	863.26	9.50E-05	701.7
1.00E-04	792.67	1.00E-04	738	1.00E-04	641.25